

An-Najah National University

Faculty of Graduate Studies

**ZnO/Montmorillonite Nanoparticles as Photo-degradation
Catalyst and Adsorbent for Tetracycline in Water: Synergic
Effect in Supported System**

By

Najat Maher Nemer Aldaqqa

Supervisors

Prof. Hikmat S. Hilal

Dr. Waheed J. Jondi

**This Thesis is Submitted in Partial Fulfillment of the Requirements for
the Degree of Master of Science in Chemistry, Faculty of Graduated
Studies, An-Najah National University, Nablus, Palestine.**

2014

**ZnO/Montmorillonite Nanoparticles as Photo-degradation
Catalyst and Adsorbent for Tetracycline in Water: Synergic
Effect in Supported System**

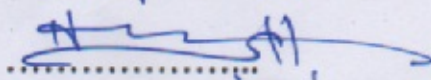
By
Najat Maher Nemer Aldaqqa

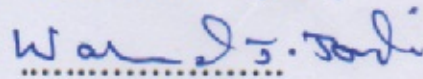
This Thesis was defended successfully on 18 /09/2014 and approved by:

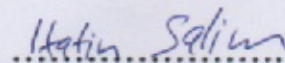
Defense Committee Members

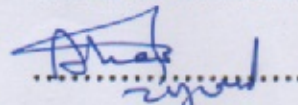
1. Prof. Hikmat S.Hilal / Supervisor
2. Dr. Waheed J.Jondi / Co-Supervisor
3. Dr. Hatim Salim / External Examiner
4. Dr. Ahed Zyoud / Internal Examiner

Signature


.....


.....


.....


.....

DEDICATION

I dedicate this thesis to my parents , who taught me to trust in Allah, believe in hard work, supporting and encouraging me to believe in myself.

To my brothers who try to make me feel happy all time.

To my beloved betrothed Mohanad Alian for his support, which give me the courage and confidence.

Acknowledgements

First of all, I thank Almighty God who gave me the ability to complete my work. I would like to express my sincere gratitude to my research supervisors Professor Dr .Hikmat Hilal and Dr Waheed Jondi for their guidance, suggestions and support given to me in completing the thesis. Their timely help and motivation are also remembered .

I would like to thank Dr Ahed zyoud for his constant support and giving me ideas for interpreting the experimental results. Thanks to all other teachers of An-Najah National University. Thanks to the technical staff at the Department of Chemistry at An-Najah National University, especially Mr. Omair Al-Nabulsi and Mr. Nafeth Dwekat. I would like to thank Mr. Wassem Mansour for his assistance and scientific advice. I would to acknowledge the Industrial Co., LTD. #1239-5, South Korea for kindly conducted measurements of XRD.

I am grateful to General American Consulate in Jerusalem for providing me master scholarship award. I am obliged to my colleagues and dear friends, especially Julnar Masharqah, Haneen Hanaishi for all their support, motivation, and help. Finally, I express my happiness to my parents, brothers and my betrothed Mohanad for giving me love, guidance, confidence and endless support.

أنا الموقع أدناه مقدم الرسالة التي تحت عنوان:

**ZnO/Montmorillonite Nanoparticles as Photo-degradation Catalyst
and Adsorbent for Tetracycline in Water: Synergic Effect in
Supported System**

دراسة التأثير المتبادل لحبيبات أكسيد الزنك النانوية المثبتة على المنتموريالونيت وعملها
كحفاز للتخطيم الضوئي وكما مادة ممتزة للتتراسيكلين

أقر بأن ما اشتملت عليه الرسالة إنما هي من إنتاجي الشخصي باستثناء ما تمت الإشارة إليه حيثما
ورد، وأن الرسالة ككل، أو أي جزء منها لم يقدم من قبل لنيل أية درجة علمية أو بحث علمي أو
بحثي لدى أية مؤسسة تعليمية أو بحثية أخرى.

Declaration

This work provided in this thesis, unless otherwise referenced, is the
researcher's own work, and has not been submitted elsewhere for any other
degree or qualification.

Student name:

اسم الطالب: نجاة ماهر بن الدقه

Signature:

التوقيع: نجاة الدقه

Date:

التاريخ: ١٨/٩/٢٠١٤

List of Contents

| No. | Subject | Page |
|---|---|------|
| | Dedication | iii |
| | Acknowledgments | iv |
| | Declaration | v |
| | List of Contents | vi |
| | List of Tables | ix |
| | List of Figures | x |
| | List of Abbreviations | xiii |
| | Abstract | xv |
| CHAPTER 1: INTRODUCTION | | |
| 1.1 | Overview | 1 |
| 1.2 | Tetracycline | 3 |
| 1.2.1 | Source, Use, and Chemistry of Tetracycline | 3 |
| 1.3 | Adsorption | 6 |
| 1.3.1 | Adsorption Definition and Operation | 6 |
| 1.3.2 | Adsorption Features | 6 |
| 1.3.3 | Adsorbents Used to Remove Tetracycline from Water | 7 |
| 1.4 | Clay | 7 |
| 1.4.1 | Montmorillonite | 10 |
| 1.5 | Photodegradation | 12 |
| 1.5.1 | Concept of Photodegradation | 12 |
| 1.5.2 | ZnO Semiconductor Catalyst | 14 |
| 1.6 | Composite Catalysts | 16 |
| 1.7 | Objectives | 17 |
| 1.8 | Novelty of This Work | 18 |
| CHAPTER 2: Materials and Methods | | |
| 2.1 | Chemicals | 20 |
| 2.2 | Equipments | 20 |
| 2.3 | Preparation of required Solutions | 21 |
| 2.3.1 | Stock Solutions | |
| 2.3.2 | Other Solutions | 21 |
| 2.4 | Catalyst Preparation | 22 |
| 2.4.1 | ZnO Nano-Particles | 22 |
| 2.4.2 | Preparation of ZnO Particles Entrapped in Montmorillonite | 22 |
| 2.5 | Photo-Catalytic System and Irradiation Sources | 23 |
| 2.5.1 | Photo-catalytic System | 23 |
| 2.5.2 | Effect of Catalyst Amount | 24 |
| 2.5.3 | Effect of Tetracycline Concentration | 24 |

| | | |
|--|--|----|
| 2.5.4 | Effect of pH | 24 |
| 2.5.5 | Control Experiments | 25 |
| 2.6 | Adsorption Experiments | 26 |
| 2.6.1 | Effect of annealing of adsorbent | 26 |
| 2.6.2 | Effect of Temperature | 27 |
| 2.6.3 | Effect of pH | 27 |
| 2.6.4 | Effect of Contact Time | 27 |
| 2.6.5 | Effect of Tetracycline Concentration | 27 |
| 2.6.6 | Control Experiment for adsorption Study | 28 |
| 2.6.7 | Equilibrium Isotherm Models | 28 |
| 2.6.7.1 | Langmuir Adsorption Isotherm | 28 |
| 2.6.7.2 | Freundlich Adsorption Isotherm | 29 |
| 2.6.8 | Adsorption Kinetic Models | 30 |
| 2.6.8.1 | Pseudo-First Order Kinetics | 31 |
| 2.6.8.2 | Pseudo Second-Order Kinetics | 31 |
| 2.6.8.3 | Intra-particle Diffusion Model | 32 |
| 2.7 | Tetracycline Desorption Experiments | 32 |
| 2.8 | Calibration Curve | 32 |
| CHAPTER 3: RESULTS AND DISCUSSION | | |
| 3.1 | Catalysts Characterization | 35 |
| 3.1.2 | Photoluminescence (PL) Spectra of ZnO | 35 |
| 3.1.2 | Photoluminescence (PL) Spectra of Montmorillonite and Composite Material | 36 |
| 3.1.3 | ZnO XRD Characterization | 37 |
| 3.1.4 | XRD Pattern for Montmorillonite | 39 |
| 3.1.5 | XRD Pattern of ZnO/Montmorillonite | 40 |
| 3.2 | Tetracycline Adsorption Experiments | 43 |
| 3.2.1 | Effect of Adsorbent Type | 43 |
| 3.2.2 | Effect of Tetracycline Concentration | 46 |
| 3.2.3 | Effect of pH | 47 |
| 3.2.4 | Effect of Temperature on Adsorption | 50 |
| 3.2.5 | Kinetics of Tetracycline Adsorption | 51 |
| 3.2.7 | Adsorption Isotherms | 57 |
| 3.3 | Tetracycline Photo- Degradation Studies | 60 |
| 3.3.1 | Commercial ZnO Catalyst System | 63 |
| 3.3.1.1 | Effect of ZnO Catalyst Amount | 63 |
| 3.3.1.2 | Effect of Tetracycline Concentration | 67 |
| 3.3.1.3 | Effect of pH on Degradation of Tetracycline | 69 |
| 3.3.1.4 | Effect of ZnO Catalyst Type | 71 |
| 3.3.2 | ZnO/Montmorillonite Photo-Catalysis System | 73 |
| 3.3.2.1 | Effect of pH on Photo-degradation | 77 |

| | | |
|------------|--|----|
| 3.4 | Recovery of ZnO/Montmorillonite Material | 78 |
| | CONCLUSION | 80 |
| | Recommendations for Future Works | 82 |
| | REFERENCES | 84 |
| | الملخص | ب |

List of Tables

| No. | Subject | Page |
|------|--|------|
| 1.1 | Daily approved human dose and metabolism of the target antibiotics. | 2 |
| 3.1 | The percentage removal of Tetracycline by different types of adsorbent after 100 min adsorption. | 45 |
| 3.2 | The percentage removal of Tetracycline with time by using non-annealed ZnO/Montmorillonite for 120 min adsorption. | 46 |
| 3.3 | The correlation coefficients and other parameters measured for pseudo- first- order kinetic and pseudo-second-order kinetic models. | 55 |
| 3.4 | Intra-particle diffusion model parameters for Tetracycline adsorption onto Montmorillonite and ZnO/ Montmorillonite at 25°C. | 56 |
| 3.5 | Adsorption isotherm models coefficients for Tetracycline adsorption. | 60 |
| 3.6 | Values of percentage of degradation, turnover number (TN), turnover frequency (TF) and quantum yield (QY) measured for Tetracycline degradation by changing ZnO amount after 15 min. | 66 |
| 3.7 | Values of % degradation, turnover number (TN), turnover frequency (TF) and quantum yield (QY) measured for Tetracycline degradation after 15 min using different Tetracycline concentration. | 68 |
| 3.8 | Values of % degradation, turnover number (TN), turnover frequency (TF) and quantum yield (QY) measured for Tetracycline degradation after 15 min at different pH mediums | 71 |
| 3.9 | Values of percentage degradation, turnover number (TN), turnover frequency (TF) and quantum yield (QY) measured for Tetracycline degradation after 15 min using different ZnO type. | 73 |
| 3.10 | Values of percentage of photo-degradation, turnover number (TN), turnover frequency (TF) and quantum yield (QY) measured for TC degradation after 15min with different type of composite catalyst. | 76 |
| 3.11 | Values of percentage photo-degradation, turnover number (TN), turnover frequency (TF) and quantum yield (QY) measured for Tetracycline degradation by non-annealed ZnO/Montmorillonite after 15 min in different pH media. | 78 |
| 3.12 | Efficiency of recovered non-annealed ZnO/Montmorillonite in photo-degradation reaction of Tetracycline. | 79 |

List of Figures

| No. | Subject | Page |
|-------------|--|------|
| 1.1 | Examples of Tetracyclines. a) Doxycycline and b) Minocycline | 4 |
| 1.2 | Tetracycline structural formula. | 4 |
| 1.3 | Structure of a) apoterramycin and b) isotetracycline. | 5 |
| 1.4 | Basic structures of clay minerals, a) Octahedral sheets and b) Tetrahedral sheets | 8 |
| 1.5 | Structural of different type of clay | 9 |
| 1.6 | Montmorillonite layered structural | 10 |
| 1.7 | Photo-catalysis reaction after light radiation | 13 |
| 2.1 | Atypical calibration curve for Tetracycline in Distilled Water by UV-Vis spectrometric method | 33 |
| 2.2 | Atypical calibration curve for Tetracycline in DMSO by UV-Vis spectrometric method | 34 |
| 3.1 | Photoluminescence spectra measured for commercial ZnO powder. (Baseline made on distilled water). | 35 |
| 3.2 | Photoluminescence of a) ZnO/ Montmorillonite and b) Montmorillonite clay minerals. | 36 |
| 3.3 | X-ray diffraction pattern for commercial ZnO powder. | 37 |
| 3.4 | X-ray diffraction pattern for prepared ZnO powder. | 38 |
| 3.5 | X-ray diffraction pattern for Montmorillonite. | 39 |
| 3.6 | X-ray diffraction pattern for prepared ZnO/Montmorillonite composite material. | 40 |
| 3.7 | X-ray diffraction pattern for prepared N ₂ -annealed ZnO/Montmorillonite composite material. | 41 |
| 3.8 | X-ray diffraction pattern for prepared air-annealed ZnO/Montmorillonite composite material. | 42 |
| 3.9 | Percentage of Tetracycline removal by different types of adsorbent, a) non-annealed b) annealed with air c) annealed with N ₂ d) Montmorillonite e) air- annealed Montmorillonite at (initial conc.:120 mg/L, temperature: 25 °C, 0.1g of adsorbent in a neutral medium). | 43 |
| 3.10 | Effect of Tetracycline initial concentration on the adsorption process at (temperature: 25°C, amount of non-annealed ZnO/ Montmorillonite adsorbent 0.1 g at pH=7). | 46 |
| 3.11 | Amount of Tetracycline removal variation with changing initial concentration of Tetracycline after 120 min using (0.1 g non-annealed ZnO/ Montmorillonite adsorbent, temperature: 25°C and pH=7). | 47 |
| 3.12 | Structure of Tetracycline | 48 |
| 3.13 | Speciation of Tetracycline under different pH values (TC: | 49 |

| | | |
|-------------|--|----|
| | Tetracycline and TCH_3^+ means protonated Tetracycline) | |
| 3.14 | Effect of pH on Tetracycline removal by non-annealed ZnO/Montmorillonite adsorbent with contact time at (initial concentration 80 ppm, temperature 25°C and 0.1g ZnO/Montmorillonite adsorbent). | 49 |
| 3.15 | Effect of temperature on adsorption of 100 mL solution Tetracycline (120 ppm) using 0.10 g of non-annealed adsorbent at: a) 25°C b) 40°C c) 55°C d) 75°C. For better temperature control, adsorption process was conducted using thermostated water bath for 120 min at pH=7. | 51 |
| 3.16 | Percentage removal of Tetracycline by adsorption with a) Montmorillonite b) non-annealed ZnO/Montmorillonite at 0.1 g adsorbent, 120 ppm Tetracycline, pH=7 at room Temperature). | 52 |
| 3.17 | Kinetics of Tetracycline removal according to the pseudo-first-order model by non-annealed Montmorillonite/ZnO and nicked Montmorillonite at (initial concentration: 80 ppm, pH=7, temperature: 25 °C and 0.1g adsorbent). | 53 |
| 3.18 | Kinetics of Tetracycline removal according to the pseudo-Second – order model by Montmorillonite/ZnO and nicked Montmorillonite at (initial concentration: 80 ppm, pH: 7, temperature: 25 °C and 0.1 g adsorbent). | 53 |
| 3.19 | Kinetics of Tetracycline removal according to the intra-particle diffusion model by Montmorillonite/ZnO and nicked Montmorillonite at (initial concentration: 80ppm, temperature: 25 °C and 0.1g adsorbent). | 54 |
| 3.20 | Equilibrium adsorption isotherm of Tetracycline onto non-annealed ZnO/Montmorillonite adsorbent at 25°C and neutral medium. | 57 |
| 3.21 | Freundlich plot for Tetracycline adsorption onto non-annealed adsorbent at 25°C and neutral medium. | 58 |
| 3.22 | Langmuir plot for Tetracycline adsorption onto not annealed adsorbent at 25°C and neutral medium | 59 |
| 3.23 | Absorption spectra of Tetracycline solution in distilled water in a neutral pH at room temperature. | 61 |
| 3.24 | Spectro-photometric spectra of the photo-degradation of tetracycline in the presence of ZnO photo-catalyst. Here, Absorbance of peak at 365 nm disappeared completely after 75 min at: 40 ppm Tetracycline, 0.1 g ZnO, room temperature and neutral pH medium under simulated solar light. | 62 |
| 3.25 | Effect of ZnO catalyst amount on degradation of Tetracycline at: solution concentration: 40 ppm Tetracycline, temperature: 25°C, 0.1 g ZnO and neutral pH medium under simulated solar light. | 64 |

| | | |
|-------------|--|----|
| 3.26 | Effect of ZnO catalyst amount on Turnover number of Tetracycline degradation, at: solution concentration: 40 ppm Tetracycline, temperature: 25°C, 0.1 g ZnO and neutral pH medium under simulated solar light. | 66 |
| 3.27 | Effect of Tetracycline concentration on photo-degradation reaction: a) 10 ppm b) 20 ppm c) 30 ppm d) 40 ppm. By using 0.10 g ZnO in 100 mL solution and neutral pH at room temperature under direct solar light. | 67 |
| 3.28 | Effect of Tetracycline Concentration on Turnover number of degradation at catalyst amount: 0.1g, contact time: 15 min, pH = 7 and temperature: 25°C under simulated solar light. | 69 |
| 3.29 | Effect of pH on degradation of Tetracycline with using (commercial ZnO powder catalyst amount: 0.1 g, Tetracycline concentration: 40 ppm, and temperature: 25°C under simulated solar light. | 70 |
| 3.30 | Effect of ZnO types with time on degradation of Tetracycline at (catalyst amount: 0.1g, Tetracycline concentration: 40 ppm, pH=7 and temperature: 25°C under simulated solar light. | 72 |
| 3.31 | Adsorption and photo-degradation of Tetracycline by using non-annealed ZnO/Montmorillonite composite material at (catalyst amount: 0.1g, initial Tetracycline concentration: 120 ppm, pH=7 and temperature: 25°C under simulated solar light). | 73 |
| 3.32 | Photo-degradation of Tetracycline by different catalysts after adsorption equilibrium using (catalyst amount 0.1g, initial Tetracycline concentration 120 ppm, pH=7 and temperature 25°C under simulated solar light). | 75 |
| 3.33 | Effect of pH on degradation of Tetracycline with contact time using (non-annealed ZnO/Montmorillonite catalyst amount: 0.1 g, Tetracycline concentration: 120 ppm, and temperature: 25°C under simulated solar light. | 77 |

List of Abbreviations

| Symbol | Abbreviation |
|------------------|--|
| AOPs | Advanced Oxidation Processes |
| UV | Ultra violet |
| E_g | Band Gap |
| XRD | X-ray Diffraction |
| e^- | Electron |
| h^+ | Hole |
| VB | Valance Band |
| CB | Conduction Band |
| PL | Photoluminescence |
| TF | Turnover Frequency |
| TN | Turnover Number |
| QY | Quantum Yield |
| Ppm | Part Per million (mg/L) |
| Λ | Wavelength |
| Θ | Theta |
| Å° | Angstrom |
| Nm | Nano-meter |
| eV | Electron Volt |
| w/cm^2 | Watt pr square centimeter |
| TC | Tetracycline |
| INT | Intensity |
| q_e | Amount of adsorbate per unit mass of adsorbent at equilibrium |
| Q_o | Langmuir constant related to the adsorption capacity at equilibrium |
| C_e | The equilibrium concentration of the adsorbate |
| B | Langmuir affinity constant related to the rate of adsorption |
| K_F | Freundlich constant related to adsorption capacity |
| N | Freundlich constant provides an indication of how favorable the adsorption process |
| q_t | The adsorption capacity at time t (min) |
| k_1 | The rate constant of pseudo first-order Kinetic adsorption model |

| | |
|-------|---|
| k_2 | The equilibrium rate constant of pseudo second-order adsorption |
| k_p | The diffusion rate constant of Intra-particle Kinetic Model |
| C | Intra-particle diffusion constant that gives an indication of the thickness of the boundary layer |
| B | The line broadening at half the maximum height in radians of XRD peak |
| K | The shape factor (Scherrer equation) with a typical value of about 0.9 |

**ZnO/Montmorillonite Nanoparticles as Photo-degradation Catalyst
and Adsorbent for Tetracycline in Water: Synergic Effect in
Supported System**

By

Najat Maher Nemer Aldaqqa

Supervisors

Prof. Hikmat S. Hilal

Dr. Waheed J. Jondi

Abstract

Extensive use of Antibiotics in human and veterinary medicines has resulted in their frequent detection in soils, groundwater, and wastewater. Adsorption and photo-degradation are among the most effective processes used in purification of water from contaminants such as antibiotics. In this research, we studied the removal of Tetracycline, a common antibiotic, by using pristine ZnO and ZnO/Montmorillonite composite material through two processes adsorption and photo-degradation. ZnO is a semiconductor photo-catalyst that is used in photo-oxidation of contaminants under solar light to safe products. This is due to ZnO catalyst having low cost, demanding mild reaction conditions, and having high photo-catalytic activity.

Montmorillonite, a clay mineral with distinctive physical properties, was known as a good adsorbent of Tetracycline in earlier works. In this work, ZnO was supported on the surface of Montmorillonite, and the composite was used as photo-catalyst under simulated solar light. Adsorption property of this composite material was also studied. XRD and

photoluminescence spectra were used to characterize the commercial ZnO, prepared ZnO and prepared ZnO/Montmorillonite.

Adsorption process of Tetracycline on ZnO/Montmorillonite was investigated under different conditions such as pH, contact time, amount of Tetracycline, annealing and reaction temperature. Kinetics and adsorption isotherms were studied. The results showed that the adsorption process on a prepared non-annealed ZnO/Montmorillonite followed Langmuir isotherm model with adsorption capacity 112.36 mg/g in neutral pH. The adsorption capacity of non-annealed composite material is two fold higher than that for naked Montmorillonite. Most effective adsorption was found in neutral pH medium. Adsorption on both ZnO/Montmorillonite and naked Montmorillonite followed pseudo second order kinetic model.

The photo-degradation reaction of Tetracycline was investigated by using commercial ZnO photo-catalyst under different reaction conditions. Under basic conditions, the commercial ZnO showed higher photo-degradation activity under simulated solar light. Effects of different reaction conditions onto photo-degradation reaction of Tetracycline by ZnO/Montmorillonite catalyst were also studied. The higher degradation was achieved in a neutral medium.

Chapter 1

Introduction

1.1 Overview

Since the 1940s, antibiotics have played an important role in human and veterinary medicines for disease treatment [1, 2]. They are responsible for saving millions of human lives and largely used in animal operations for growth promotion and for disease prophylaxis.

The US National Library of Medicine says that antibiotics (powerful medicines that fight bacterial infections) can save lives when used properly [3]. Antibiotics either stop bacteria from reproducing or kill them [2].

Many antibiotics involve natural compounds produced and isolated from living organisms such as *Penicillium*. Most modern antibacterials are semisynthetic modifications of various natural compounds such as beta-lactam antibiotics. Synthetic antibiotics (e.g. Quinolones) are produced exclusively by chemical processes.

Different types of antibiotics affects different types of bacteria in several ways. Some antibiotics can be used to treat a wide range of infections and are known as 'broad-spectrum' antibiotics . Others are only effective against a few types of bacteria and are called 'narrow-spectrum' antibiotics.

Antibiotics transfer to the aquatic environment in the parent compound or in conjugated forms then may persist or transport to the water supply. The

potential presence of antibiotics in the environment and water ways via different pathways, including wastewater effluent discharge, run off from land to which agricultural or human waste is known [4]. It is estimated that about 75% of all antibiotics given to animals are not fully digested and eventually pass through the body and enter the environment [5]. Table 1.1 shows a significant fraction of the antibiotic dosage passes through the body which is unmetabolized and thus enters into sewage treatment plants intact.

Table 1.1: Daily approved human dose and metabolism of the target antibiotics [6].

| Antibiotic | Daily Dose (mg) | %Extraction Unchanged |
|-------------------------|----------------------------|----------------------------------|
| Sulfamethoxazole | 2000 | 20-40 |
| Trimethoprim | 160 | 25-60 |
| Ciprofloxacin | 200 | 25-50 |
| Tetracycline | 500 | 80-90 |

Varieties of antibiotics have been detected in wastewater effluents and natural waters at ng/L to low $\mu\text{g/L}$ levels [7]. The presence of antibiotics in source drinking water is of concern due to the unknown health effects of chronic low-level exposure to antibiotics over a lifetime if the antibiotics survive drinking water treatment and are present in consumer's drinking water.

In recent times, advanced oxidation processes (AOPs) have been established for the purification of water from many contaminants. By applying AOPs, complete oxidation of organic pollutants into CO_2 and H_2O

will be achieved. The application of AOPs in heterogeneous photocatalysis is highly promising to treat non-biodegradable toxic organic molecules that exist in water [8].

1.2 Tetracycline

1.2.1 Source, Use, and Chemistry of Tetracycline

In the late of 1940, Tetracyclines were discovered as a family of antibiotics and were accepted to treat a broad spectrum of bacterial infections [1, 9]. They are widely produced and applied in livestock farming for treating animal diseases and encouraging growth rate [10]. Tetracycline antibiotics have a very broad spectrum of actions, and can be used to treat mild acne, urinary tract infections, Rocky Mountain spotted fever, upper respiratory tract infections, sexually transmitted diseases, Lyme Disease and typhus [11, 12].

The most commonly prescribed Tetracyclines are :

1. Tetracycline
2. Doxycycline
3. Minocycline

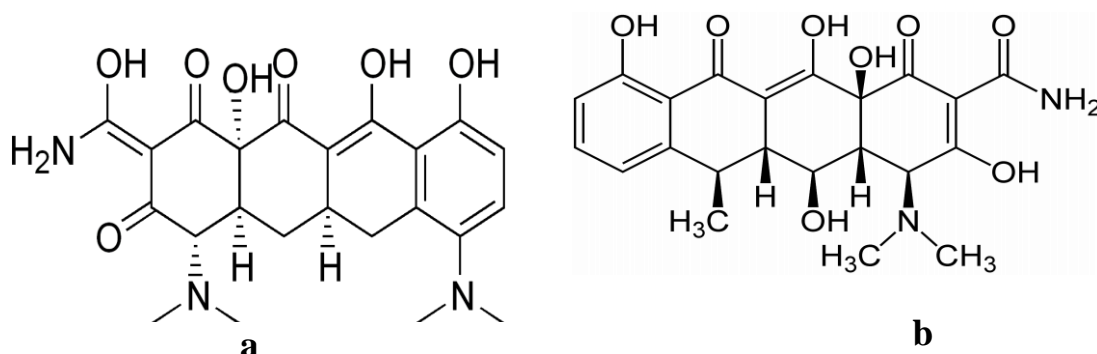


Figure 1.1: Examples of Tetracyclines. a) Doxycycline and b) Minocycline

Tetracyclines antibiotics have the potential to arrive at soil and aquatic environment [13]. Residues of Tetracycline have been frequently detected in waste water [4, 7, 14], sediments [15], groundwater [16] and surface water [14]. Exposure to low-level antibiotics and their transformation products in the environment could be poisonous and cause spreading of antibiotic resistant genes between microorganisms. Information about the environmental transfer and fate of Tetracycline is still limited [10].

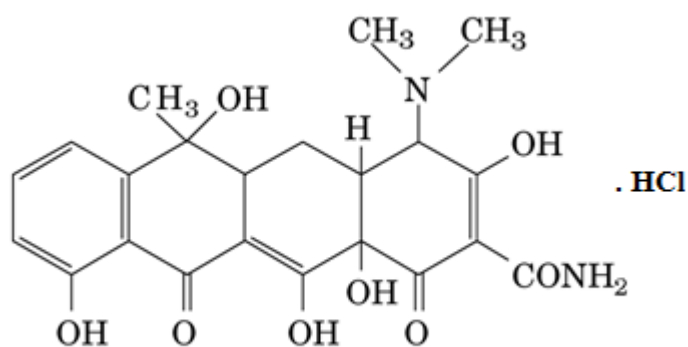


Figure 1.2: Tetracycline structural formula.

Currently, the name "Tetracycline" ($C_{22}H_{25}ClN_2O_8$) was derived from a system of four linearly annelated six-membered rings (4S,4aS,5aS,6S,12aS)-4-(Dimethylamino)-3,6,10,12,12a-pentahydroxy-6-methyl-1,11-dioxo-1,4,4a,5,5a,6,11,12a-octahydrotetracene-2-carboxamide

hydrochloride) or (1,4,4a,5,5a,6,11,12a-octahydronaphthacene) with a characteristic arrangement of double bonds. It exists as yellow crystalline powder at room temperature. It is soluble in water, ethanol, 2-propanol and DMSO [17]. Determination of the crystal structure of Tetracycline hydrochloride has clearly defined the stereochemistry of each carbon atom centers [18]. Due to the functionality and the sensitivity nature of Tetracycline, the reactions that undergo are usually of a complicated nature. In Acidic conditions, Tetracycline undergoes dehydration to yield anhydrotetracycline. However, in Basic conditions, Tetracycline is transformed to isotetracycline.

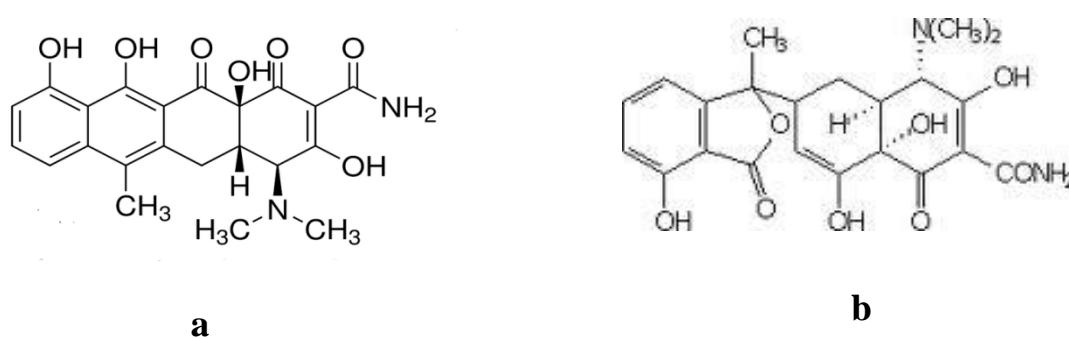


Figure 1.3: Structure of a) anhydrotetracycline and b) isotetracycline [18].

As described in Table 1.1, It is estimated that about 80-90% Tetracycline presence in the environment and waterways via different pathways and thus enters into sewage treatment plants intact. Due to unknown fate of Tetracycline molecules and residues in water, this work studied the remove of Tetracycline from water.

1.3 Adsorption

1.3.1 Adsorption Definition and Operation

Adsorption is a surface phenomenon, which includes the transfer of the solute from the solution to the surface of a contact solid material [19]. When adsorbable solute is exposed to a highly porous solid surface, a new intermolecular forces of attraction between solid and liquid cause deposition of some of the solute molecules at the solid surface. Adsorbate is a term that describes the solute retained on the solid surface, whereas, adsorbent is the solid that adsorbs other species.

Adsorption processes are classified into two types according to the nature of attractive forces between adsorbent and adsorbate. Physisorption occurs when the weak Van Der Waals forces attract the molecules. Chemisorption process happens when a real chemical bond forms between the solute and solid surface (such as covalent bond).

1.3.2 Adsorption features

Adsorption is an extremely important process of utilitarian significance. It has a practical application in technology, environmental protection, biological and industrial fields [20]. In many catalytic reactions, adsorption of a substrate is the first stage of the process [21]. Moreover, adsorption is also one type of methods that used for separation of the mixtures in the laboratory [22]. On the other hand, adsorption process is of vital importance in purification. Adsorption is gaining attention as one of

the most useful processes for treatment of industrial effluent containing toxic materials and removing them from water, soil and air [23].

The major advantages of adsorption over conventional treatment methods include:

1. Low cost
2. Simplicity
3. High efficiency
4. Minimization of chemical and biological waste
5. Regeneration of adsorbate
6. Possibility of adsorbent recovery
7. Successful operation over a wide range of pH and temperature.

1.3.3 Adsorbents Used to Remove Tetracycline from Water

Different adsorbents were widely used to remove Tetracycline from water such as: clay [24], Montmorillonite [25, 26], kaolinite [26], soil [27, 28], carbon nanotubes [29], Graphene oxide [30], borosilicate glass [31], aluminum oxide [32], hydroxyapatite [33], humic-mineral complexes [34], chitosan particles [35], goethite [36] and palygorskite [37].

1.4 Clay

Clay is an abundant natural material in the earth crust. It is a class of Phyllosilicates which mostly involve fine-grained minerals (less than 2 μm) [38]. Clay involve hydrous silicates, largely of magnesium, aluminum, and

iron [39]. Chemically, clays have colloidal layered aluminosilicates $[\text{Al}_4\text{Si}_4\text{O}_{10}(\text{OH})_8]$ and hold negative charges [40]. It has affinity to adsorb water and other polar fluids due to this negative charge on its surface [40].

The basic structure of clay minerals can be obtained according to the stacking of two sheets: a sheet of corner-linked tetrahedra and a sheet of edge-sharing octahedra sometime separated by an interlayer. Different types of clay minerals are formed by (1) different combinations of these two units and the interlayer space and (2) type of cations between layers such as (Mg^{+2} , Fe^{+2} , Na^+ and K^+). The linkage of atoms in tetrahedral and octahedral sheets was illustrated in Figure 1.4.

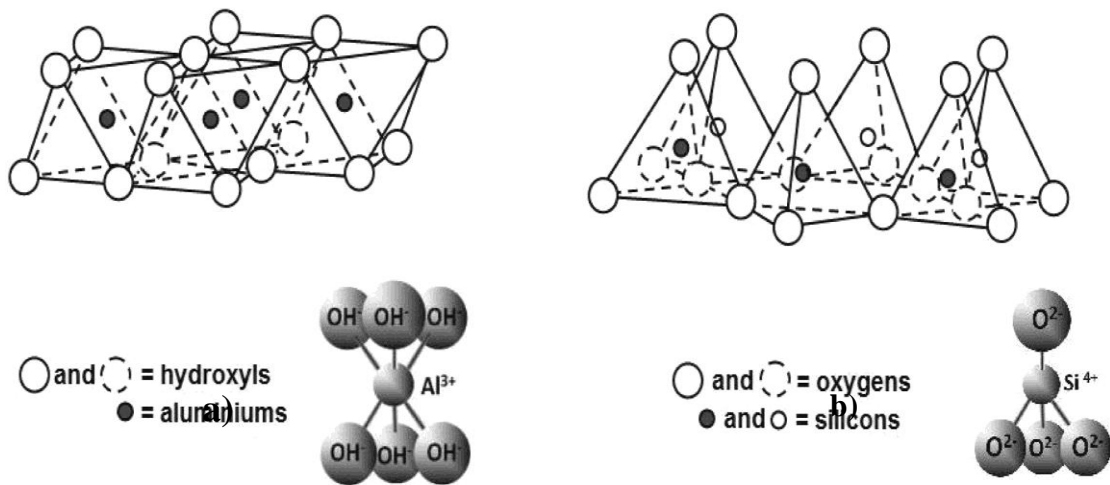


Figure 1.4: Basic structures of clay minerals, a) Octahedral sheets and b) Tetrahedral sheets [41].

The important clay mineral groups are Kaolinites, Chlorite, Smectites, Illitesm, Vermiculites and Kaolin. The most frequent clay minerals found in nature are Kaolinite from the Kaolin group and Montmorillonite from the smectite group [38].

Based on Figure 1.5, clay minerals can be classified as 1:1 or 2:1, when one tetrahedral sheet is bonded to one octahedral sheet, a 1:1 clay mineral is produced as kaolinite. The electronegativity and capacity of kaolinite clay units to adsorb cations is due to the surface and broken OH -edge groups. A 2:1 clay consists of an octahedral sheet sandwiched between two tetrahedral sheets, and example is Montmorillonite. 2:1 clays can be classified into non-expanding (Illite and micas) and expanding (smectites) clays.

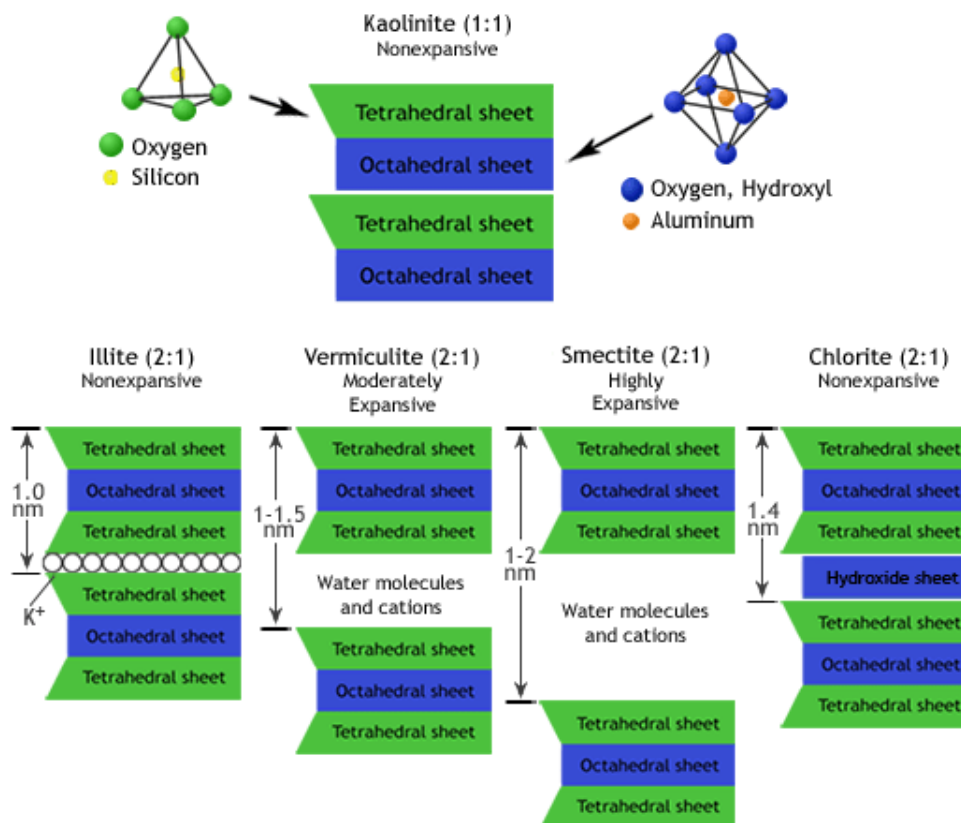


Figure 1.5: Structural of different type of clay [42].

For example, in a 1:1 clay mineral layer, such as kaolinite, clay mineral would have one tetrahedral and one octahedral sheet per clay layer (Figure

1.5). Clay is known for surface activity, which depends to different degrees on their crystal structures and according to the size, charge and structure of the adsorbate [43, 44]. Organic molecules may interact or adsorb on clay particles in several ways: by dispersion forces, ion-dipole forces or by hydrogen bonding [43].

1.4.1 Montmorillonite

Montmorillonite, which is a member of smectites clay minerals (2:1 minerals), typically forms microscopic or tiny platy micaceous crystals. The theoretical formula is $(\text{OH})_4\text{Si}_8\text{Al}_4\text{O}_{20}\cdot n\text{H}_2\text{O}$. Due to the high cation-exchange capacities and the interlayer spacing of Montmorillonite, the water content is variable and occurs between their layers. In addition to being involved in inorganic exchange reactions, Montmorillonite react with and adsorb some organic molecules through hydrogen bonding, such as amines, glycols, glycerols, and other polyhydric alcohols [45].

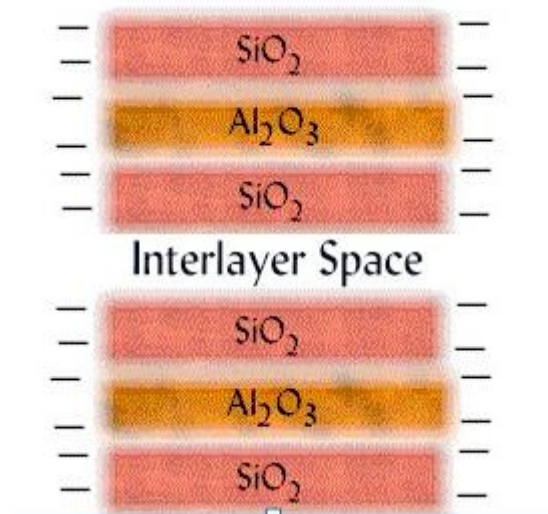


Figure 1.6: Montmorillonite layered structural.

Montmorillonite has been considered as a potential adsorbent toward heavy metals [46], organic herbicides [47], dyes [48, 49], antibiotics [50, 51] and others. Organo -Montmorillonite is a complex, which is formed by adsorbing organic compounds on Montmorillonite. The adsorption mechanism and how strongly the molecules are bonded to Montmorillonite depend on the type, structure and number of polar functional groups present in the organic compound.

Montmorillonite carries a negative charge that attracts the positively charged molecules. Thus, Montmorillonite adsorbs cationic molecules mainly by electrostatic forces. Nonionic organic compounds are also adsorbed by Montmorillonite, but the adsorption is due to hydrogen bonding and van der Waals' attraction forces. However, inorganic anions are adsorbed at the positive sites on the edges of Montmorillonite crystals. The degree of adsorption at these sites would be relatively minor as compared to cationic adsorption [52].

This adsorptive property has benefits to enforce the photo-activity of semiconductor when a photo-catalyst is immobilized on Montmorillonite. Previous studies reported photo-activity increase by dispersing catalyst, such as TiO_2 , onto Montmorillonite supports [53, 54]. Results of these investigations recommended that the high specific surface area and porous structure of Montmorillonite were useful to photo-activity via enhancing adsorption. Adsorption is believed to be the determining step in the heterogeneous photo-catalytic reactions. Therefore, a combination of

adsorption and heterogeneous photo-catalysis makes photo-oxidation or degradation more effective for the removal of contaminants from wastewater as discussed later.

1.5 Photo-degradation

1.5.1 Concept of Photo-degradation

In the early 1970's, the Photo-catalysis phenomenon attracted a special attention after Fujishima and Honda discovered the photolysis of water by a photo-catalyst [55-57]. It is a promising phenomenon for many applications of solar light. Photo-catalysis was defined as the "*speeding up of the photoreaction by the presence of a catalyst.*" A catalyst is "*a substance, which accelerates a reaction by providing a new path with lower activation energy without being consumed in the reaction process*".

There are two classes of photo-catalysis processes according to the phase of photo-catalyst used. In a homogeneous photo-catalysis, the reaction medium and catalyst are in the same phase as photo-Fenton System. By contrast, in a heterogeneous photo-catalysis reaction the catalyst exists in the different phase from that of the reaction.

Semiconductors and some transition metal oxides, which have a continuum of electronic states, are the most frequent heterogeneous photo-catalyst. Some semiconductors (as TiO_2 , Fe_2O_3 , ZnO , ZnS and CdS) are described by a filled valence band and an empty conduction band [56].

A semiconductor is usually a solid substance that has an electrical conductivity between a conductor and an insulator. In semiconductors, the band of energy where all of the valence electrons are located and are involved in the highest energy molecular orbital is the valence band (VB), while the conduction band (CB) is the lowest unoccupied energy band.

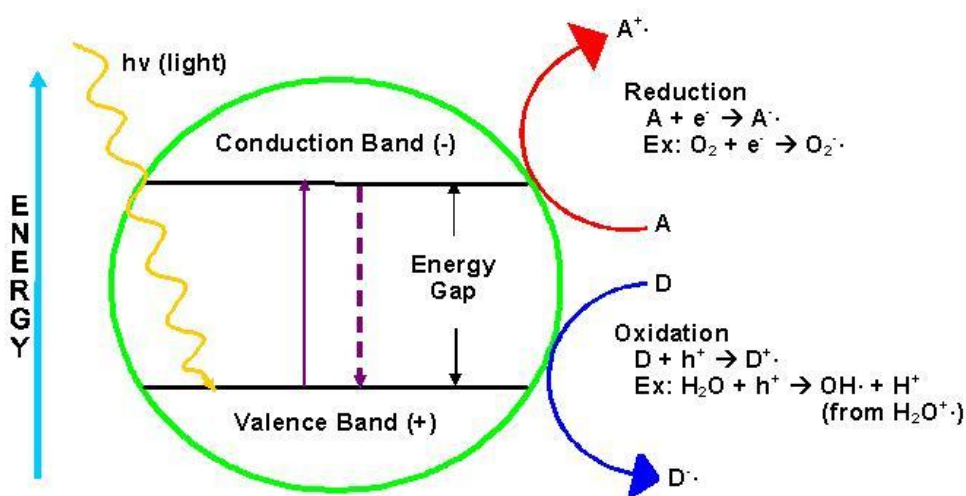


Figure 1.7: Photo-catalysis reaction after light radiation [58].

In photo-catalysis, when a photon with an energy ($h\nu$) matches or exceeds the band gap energy (E_g) of the semiconductor, an electron is elevated from the valence band into the conduction band leaving a hole (h^+) in VB (see Figure 1). Recombination of excited electron and hole may occur and release the excitation energy of the electron as radiation or heat. However, this recombination is not desirable process. Main goal of the created electron-hole pairs is to have a reaction between the holes with reducible molecules to produce an oxidized product, and a reaction between the excited electrons with oxidants to produce products through a series of possible reactions to degrade those molecules to give CO_2 and H_2O . This

oxidation-reduction reaction occurs at the surface of semiconductors. The positive holes in the oxidative reaction react with the H₂O molecules close to the surface and generate a hydroxyl radical [57].



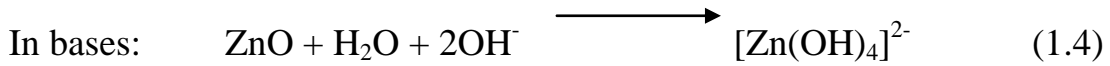
On the other hand, electrons combines with O₂ molecules to produce Superoxide ion ($\cdot\text{O}_2^-$) which is a highly reactive particle and capable to oxidize organic materials.

Semiconductors have several important applications in chemistry. For example, conversion of light to electricity, photo-catalysis of water, soil and air purification and disinfection from pesticides, herbicides, microorganisms drugs and many other pollutants.

1.5.2 ZnO Semiconductor Catalyst

Zinc oxide, which is a white inorganic fine particle powder, is almost insoluble in water but soluble in acids or bases. It is a promising substance that was used in semiconductor device applications and as an additive material in plastics, ceramics, glass, lubricants, paints, adhesives, sealants, pigments, foods (source of Zn nutrient), ferrites, batteries and others [59-61].

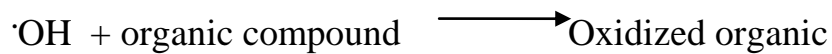
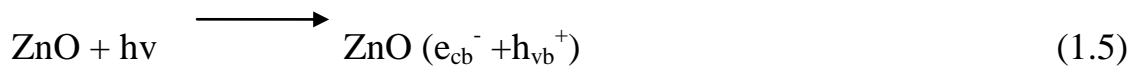
The reactions of ZnO depend on the pH value of the media, because ZnO is an amphoteric oxide. It reacts as a base in acidic solution and as an acid in basic solutions [62]



ZnO in materials science is frequently classified as II-VI semiconductor because zinc and oxygen belong to the second and sixth groups respectively in the periodic table. This semiconductor is mostly used due to [63]:

1. High photosensitivity
2. Photochemical stability
3. Wide band gap [64]
4. Strong oxidizing power
5. Non-toxic nature
6. Low cost

The band gap of ZnO is relatively large (3.2 eV at room temperature) [60], with limited photo-catalytic applications to shorter wavelengths (it demands UV light). Only about 5% of the solar spectrum falls in the UV region, so ZnO semiconductor show activity under solar light. Based on previous investigations utilizing ZnO, the disinfection mechanism can be written as a following [61, 65]:



1.6 Composite Catalysts

Composite materials are solid materials that involve two or more different substances to attain properties that the constituent materials cannot attain individually, or to increase the activity of desirable properties of one of the substances [66, 67]. In general, composite materials involve two phases: ‘reinforcements’ or ‘fillers’ and ‘Binder’ or ‘matrix’ [67]. The matrix surrounds the reinforcement and holds them in place. This concept has been known as early as 1500 B.C. Currently in chemical industry, composite catalysts are being used to meet the practical catalytic performance requirements of high selectivity, high activity, and good stability.

The main advantage of composite materials lies in their easy recovery from treated solutions. Catalyst powder diffuses in an aqueous solution, as ZnO and TiO₂ particles, and is very difficult to recover. To solve the recovery problem for these catalysts, TiO₂ and ZnO were supported on different materials to enlarge application fields and overcome recovery problems

[54, 65]. Materials with large surface area as silica, clay minerals, zeolites or activated carbons and combined metal oxides have also been used. Photo-activity of these materials has been studied for dyes such as methyl orange, acid black 1, and methylene blue [65].

The adsorption of the contaminant molecules is the main step in composite catalysis work during the equilibrium step. Then, the electron transfers from the valance band to the conduction band of catalyst and initiate the photo-catalysis reaction. Adsorption capacity enhancement of organic substrates on the supported material surface appeared to be the main advantage leading to enhance photo-degradation efficiency.

1.7 Objectives

The main purpose of this work is to purify water from organic antibiotic residues by two ways: adsorption and photo-degradation with simulator solar light, using a safe and low cost semiconducting material (ZnO). The nano- ZnO will be used in its commercial and prepared particle forms, and as a composite catalyst combined with safe supporting material (Montmorillonite). Evaluation of the process in terms of efficiency, cost, environmental and economic points of view will also be investigated. Reuse of the composite catalyst will also be investigated. Technical objectives include:

1. Preparation of nano-sized powder ZnO.
2. Characterization of the commercial and prepared nano- ZnO using XRD, photoluminescence, and other techniques.
3. Preparation of new nano-sized composite material (ZnO/ Montmorillonite) and characterize using XRD and photoluminescence.
4. Using the prepared ZnO powder in photo-degradation of Tetracycline in water with simulate solar light, and comparing with commercial ZnO.
5. Using ZnO/ Montmorillonite composite material in photo-degradation of Tetracycline with simulate solar light.
6. Studying effects of pH, contaminant concentration, annealing, catalyst concentration, temperature, and time of contact on photo-catalyst activity and photo-degradation process efficiency.
7. Studying the possibility of multiple use of the ZnO/ Montmorillonite catalyst (recovering and reusing the photo-catalyst for multiple times in photo-degradation process).

1.8 Novelty of This Work

Photo-catalysis process, which is a new promising environmental technology, has been widely investigated for removing water pollutant by degradation. In this study, Zinc oxide is a material having special features as discussed earlier. Researchers used naked ZnO as photo-catalyst to degrade many toxic and organic pollutants. In addition, others studied ZnO as photo-catalyst for degradation of Tetracycline antibiotic under UV radiations. In this work, nano-ZnO powder was applied in photo-

degradation process of Tetracycline under simulator solar light. In addition, ZnO was supported onto Montmorillonite clay, and then the adsorption and photo-degradation properties were studied. Naked Montmorillonite was known as a good adsorbent of Tetracycline in earlier work [25]. To our knowledge, this is the first work that investigates the work of ZnO/ Montmorillonite composite material in water purification from Tetracycline by adsorption and photo-degradation effects under simulated solar light.

Several efforts were proposed here to enhance ZnO photo-activity specially when supporting it on Montmorillonite. Supporting the semiconductor onto Montmorillonite will provide high efficiency due to Montmorillonite distinctive physical properties, such as large specific surface area, porous structure and exhibits good adsorb ability and cation exchange capacity which permits the intercalation of cationic antibiotics [65] and reduce the cost. It was reported that ZnO was intercalated into the interlayer space of Montmorillonite and also adsorbed on the surface of Montmorillonite [68].

Chapter 2

Materials and Methods

2.1 Chemicals

Commercial zinc oxide powder was purchased from Sigma Aldrich Co. ZnCl_2 (purchased from Chem. Samuel) and NaOH (from Frutarom Co.) were used for ZnO nanoparticle preparation. Zinc acetate dihydrate [$\text{Zn}(\text{OOCCH}_3)_2 \cdot 2\text{H}_2\text{O}$] from sigma Aldrich was used for composite catalyst preparation. Montmorillonite (Aluminum Pillared Clay), with surface area $250 \text{ m}^2/\text{g}$, was purchased from Sigma-Aldrich Co. Dimethyl sulfoxide (DMSO) was purchased (from sigma-Aldrich Co.). Tetracycline hydrochloride was kindly donated from Birziet- Palestine Pharmaceutical Company in a pure form.

2.2 Equipments:

A Shimadzu UV-1601 spectrophotometer was used to study the effect of Tetracycline adsorption and degradation by measuring the change in absorbance. It is equipped with a thermal printer Model DPU-411-040, type 20BE. An ICE 3000 Atomic Absorption spectrometer was used to determine the exact amount of Zn in solution through the composite catalyst preparation by using flame and Hollow Cathode Lamp of Zn. Then, the percentage of ZnO, which supported into the Montmorillonite, was calculated. A Perkin-Elmer (LS50) Luminescence Spectrometer was

used for catalyst characterization. A Lux-meter (Lx-102 light meter) was used to determine the intensity of lamp radiation.

A Scientific Ltd model 1020 D.E. centrifuge was used to prepare the aliquot for analysis. The accurate masses of chemicals were measured by using four degenerate balance AR-3130 from OHAUS Crop. The solar simulator lamp (LUXTEN) was used as a source of the visible light irradiation. Lindberg Hevi-Duty Control Tube Furnace was used for annealing the composite materials. Crystal structure and crystallinity of ZnO and other solid materials were investigated by PANalytical X'Pert PRO X-ray diffractometer (XRD), where Cu K α rays was used. The measurements of XRD were kindly conducted in Industrial Co., LTD. #1239-5, South Korea.

2.3 Preparation of Required Solutions

2.3.1 Stock Solutions

1. A Tetracycline stock solution (1000 ppm) was prepared by dissolving 0.100 g Tetracycline in distilled water and then diluted to 100.01 mL. Different solutions 20, 30, 40, 50, 60, 80, 120 ppm were prepared using a stock solution.
2. The Tetracycline stock solution (1000 ppm) was prepared by dissolving 0.100 g Tetracycline in dimethyl sulfoxide (DMSO) and then diluted to 100.01 mL.

2.3.2 Other Solutions

The following solutions were required and prepared.

1- Sodium hydroxide NaOH (0.9 M) solution was prepared by dissolving 9.000g in 250.01 mL distilled water.

2- Zinc acetate (0.39 M) was prepared by dissolving 8.500 g of Zinc acetate dehydrate in 100.01 mL distilled water.

2.4 Catalyst Preparation

2.4.1 ZnO Nano-Particles

The precipitation method was used to prepare ZnO nanoparticles. In 500.01 ml flask, 250.01 ml of Sodium hydroxide solution (0.9 M) was poured and heated at about 55 °C. Then 250.01 ml of zinc chloride solution (0.45 M) was added drop wise (in about 40 minutes) to the heated solution under high speed stirring (magnetically). The resulting powder was decanted and washed with water until the solution became neutral. The powder was then separated from the mixture using a centrifuge (speed 500 rounds per minute, for 6 min).

2.4.2 Preparation of ZnO Particles Entrapped in Montmorillonite

ZnO was supported on Montmorillonite. Clay (10.000 g) was suspended in 250 mL of 0.9 M sodium hydroxide solution and the mixture was stirred at 55 °C for 120 min with adding drop wise 100.01 mL of 0.39 M zinc acetate solution. The resulting solid was filtered and washed continuously with

distilled water until the mother liquor was neutral. The solid was dried and calcinated at 250 °C for 1 hour and then stored.

2.5 Photo-Catalytic System and Irradiation Sources

2.5.1 Photo-Catalytic System

The light source was assembled above the sample, and the light intensity was controlled using a Lux-meter. The lamp has a high stability and an intense coverage of wide spectral range (450 to 800 nm). The average measured solar light intensity during February and March months at noontime in Nablus city was 1300 Lux (1300 Lux, 0.000190337W/cm²).

The photo-degradation reaction was carried out in a 100 mL beaker containing the catalyst and the pre-contaminated water sample with the antibiotics substance.

The beaker was placed in a thermostated water-bath to prevent instantaneous change of sample temperature. The temperature was measured through reaction time and kept constant by manipulating the water bath when needed. The reactor was continuously stirred magnetically to make a good distribution of the catalyst through the sample. The Light source was adjusted at constant distance above the reactor (70 cm).

The change in Tetracycline concentration was measured with time. Small aliquots of solution were syringed out from the reaction vessel at different

reaction times, and double centrifuged (500 round/minute for 3 minutes each time). The default temperature was 25°C temperature and the default pH was 7.

2.5.2 Effect of Catalyst Amount

The effect of catalyst amount on the photo-degradation process was studied. Different amounts of ZnO 0.050, 0.100, 0.150 and 0.200 g were mixed with a 100.01 mL of Tetracycline (40 ppm) at default temperature and pH.

2.5.3 Effect of Tetracycline Concentration

The concentration of tetracycline was changed to study its effect on degradation process. Different concentrations were prepared 10, 20, 30, 40 ppm and mixed with 0.100 g of ZnO for 75 min (the adsorption of Tetracycline on ZnO reach equilibrium after 30 min then degradation step was started).

When composite catalyst was used in degradation process, different concentrations of Tetracycline were prepared 60, 80,100,120 ppm. Before degradation process, the mixture of catalyst and Tetracycline was allowed to reach equilibrium after 2 hours of shaking in the dark.

2.5.4 Effect of pH

Degradation process was studied with changing the medium pH. Experiments were carried out using 100 ml of Tetracycline (120 ppm) with

0.100 g of composite catalyst. When using ZnO as a catalyst 100.01 mL of Tetracycline (40 ppm) was mixed with 0.100 g catalyst. The pH value was controlled by adding few drops of sodium hydroxide or hydrochloric acid as desired after adsorption reached equilibrium (At acidic medium pH= 2 and basic medium pH= 10.5).

2.5.5 Control Experiments:

1- In the absence of any catalyst, 40 ppm of Tetracycline solution (100.01 mL) was placed in the reactor under visible light with stirring for 75 min. Absorption was measured before and after exposure to light. The Tetracycline concentration did not change under irradiation with time. This means that the contaminant did not photo-degrade in the absence of catalysts.

2- In the dark, 100.01 ml of Tetracycline were stirred with 0.100 g ZnO catalyst one time and with composite catalyst another time for 75 min. The absorption spectrum was measured with time. The contaminant concentration did not change. No effect of photo-degradation property of ZnO or composite catalyst in dark place.

3- ZnO has small property to adsorb Tetracycline (~ 2%), in each time it used; the solution mixtures were kept in the dark for 30 min and measure the initial absorbance after this.

2.6 Adsorption Experiments

Adsorption experiments were performed by adding 0.100 g of the adsorbent to 100.01 ml of the Tetracycline solutions with different initial concentrations (60 to 120 mg/L) under natural conditions. The experiments were performed in a shaker for a period of 2 hours at 150 rpm using 250.01 mL Erlenmeyer flask for better mass transfer at room temperature (25°C).

The remaining concentration of Tetracycline in each sample was determined by UV-Vis spectroscopy. Aliquots were taken and centrifuged (2 times, 500 round/minute for 3 minutes) and the solution was spectrophotometrically analyzed. The adsorbed concentration of Tetracycline in the adsorbent phase was calculated according to:

$$q_e = \frac{(C_i - C_e)V}{W}$$

Where C_i and C_e are the initial and equilibrium concentrations (mg/L) of Tetracycline solution respectively; V is the volume of solution (L); and W is the mass (g) of the dry adsorbent.

2.6.1 Effect of annealing of adsorbent

Amount of composite catalyst was annealed after drying at 450°C for 1 h. The annealing process was done two times, once with air and another with N_2 gas. Each type of adsorbent was used in the Tetracycline adsorption experiment and the effect of annealing was studied with 0.100 g of

adsorbent, which was mixed with 100 mL of Tetracycline (120 ppm) at 25 °C in a neutral medium.

2.6.2 Effect of Temperature

The effect of temperature on adsorption process was investigated in the range 25-70°C. Adsorbent (0.100 g) was added to 100.01 mL of Tetracycline solution (120 mg/L) and the pH was adjusted to 7. The mixture was then shaken at the desired temperature for 2 hours.

2.6.3 Effect of pH

Adsorption of Tetracycline by the non-annealed composite catalyst was studied under different pH values. The pH was controlled by adding few drops of dilute sodium hydroxide or hydrochloric acid solutions as desired. The pH indicator measured the pH value –paper (At acidic medium pH= 2 and basic medium pH= 10.5). Tetracycline solution (100.01 mL, 120 ppm) was added to 0.100 g of adsorbent sample, and the mixture was then shaken for 2 hours at 25°C.

2.6.4 Effect of Contact Time

The effect of contact time on adsorption process was studied by measuring the absorbance of sample solution for 2 hours (every 15 min).

2.6.5 Effect of Tetracycline Concentration

The effect of Tetracycline concentration on the adsorption process was studied with time. Non-annealed adsorbent (0.100g) was mixed

with 100.01 mL of different Tetracycline concentration solutions, 60, 80, 100, 120 ppm, at 25°C on a shaker in neutral mediums.

2.6.6 Control Experiment for adsorption Study

1- Montmorillonite, annealed and non-annealed, (0.100 g) was used as an adsorbent in 100.01 mL of 120 ppm Tetracycline solution. Adsorption progress was investigated for 2 hours at 25°C in the dark.

2- 120 ppm of Tetracycline was placed in a shaker for 2 hours without adsorbent to study the change of concentration with time under otherwise similar conditions.

2.6.7 Equilibrium Isotherm Models

Analysis of the isotherm data is important to develop an equation, which accurately represents the results. This could be used for design purposes and to optimize operating procedures. The most common isotherms applied in solid/liquid systems are the theoretical equilibrium isotherms; Langmuir and Freundlich (two parameter models) [69, 70].

2.6.7.1 Langmuir Adsorption Isotherm

The Langmuir isotherm, also called the ideal localized monolayer model, was developed to represent chemisorption. The Langmuir equation relates the coverage of molecules on a solid surface to the concentration of a medium above the solid surface at a fixed temperature. This isotherm is based on the assumption that [71];

- 1- Adsorption is limited to monolayer coverage.
- 2- All surface sites are alike and can only accommodate one adsorbed molecule.
- 3- The ability of a molecule to be adsorbed on a given site is independent of its neighboring site occupancy.
- 4- Adsorption is reversible and the adsorbed molecule cannot migrate across the surface or interact with neighboring molecules.

The Langmuir equation can be written as:

$$\frac{C_e}{q_e} = \frac{1}{b Q_o} + \frac{1}{Q_o} C_e$$

where q_e is the amount of adsorbate per unit mass of adsorbent (mg/g), Q_o is the adsorption capacity at equilibrium (mg/g), C_e is the equilibrium concentration of the adsorbate (mg/L) and b is the Langmuir affinity constant (L/mg). C_e/q_e values plot vs. C_e to find the Langmuir parameters.

2.6.7.2 Freundlich Adsorption Isotherm

The Freundlich isotherm (Freundlich, 1909) was interpreted as sorption to heterogeneous surfaces or surfaces supporting sites of varied affinities. It is assumed that the stronger binding sites are occupied first and that the binding strength decreases with increasing degree of site occupation. The Freundlich isotherm can describe the adsorption of organic and inorganic compounds on a wide range of adsorbents.

According to this model, the adsorbed mass per mass of adsorbent can be expressed as:

$$\log q_e = \log K_F + \left[\frac{1}{n} \right] \log C_e$$

Where q_e is the amount of adsorbate per unit mass of adsorbent (mg/g), K_F is the Freundlich constant related to adsorption capacity (mg/g), C_e is the equilibrium concentration of the adsorbate (mg/L), n is the heterogeneity coefficient gives an indication of how favorable the adsorption process (dimensionless). $\log q_e$ values plot vs. $\log C_e$ to get the Freundlich parameters.

2.6.8 Adsorption Kinetic Models

The contact time experimental results can be used to study the rate-limiting step in the adsorption process. Several adsorption kinetic models have been established to understand the adsorption kinetics and rate-limiting step. These include pseudo-first and second-order rate model, Weber and Morris sorption kinetic model, Adam–Bohart–Thomas relation, first-order reversible reaction model, external mass transfer model, first-order equation of Bhattacharya and Venkobachar, Elovich's model and Ritchie's equation [72].

In this study, three kinetic models, which are pseudo-first order, pseudo-second order, and intra-particle diffusion models were used to fit the experimental data observed in adsorption of Tetracycline onto composite

catalyst. The model with higher correlation coefficients (r^2) value (close or equal to 1) successfully describes the kinetics of tetracycline adsorption.

2.6.8.1 Pseudo-First Order Kinetics

The pseudo-first order rate expression of Lagergren model is generally expressed as:

$$\log(q_e - q_t) = \log(q_e) - \frac{k_1}{2.303}t$$

Where q_e and q_t are the mass of adsorbate per unit mass of adsorbent at equilibrium and at time t , respectively (mg/g), k_1 is the rate constant of pseudo first-order adsorption ($L \cdot \text{min}^{-1}$). The plot of $\log(q_e - q_t)$ versus t gives a straight line for the pseudo first-order adsorption.

2.6.8.2 Pseudo Second-Order Kinetics

The pseudo-second order model is based on the assumption that the rate-limiting step may be chemical adsorption involving valence forces through sharing or exchange of electrons between the adsorbent and adsorbate. The rate equation is given by Ho as :

$$\left(\frac{t}{q_t}\right) = \frac{1}{k_2 q_e^2} + \frac{1}{q_e} (t)$$

Where k_2 is the equilibrium rate constant of pseudo second-order adsorption ($\text{mg}^{-1} \text{min}^{-1}$). The plot of t/q_t versus t should give a linear

relationship that allows the computation of a second-order rate constant, k_2 and q_e .

2.6.8.3 Intra-particle Diffusion Model

The intra-particle diffusion model is based on the theory proposed by Weber and Morris. The Weber and Morris equation is:

$$Q_t = K_p t^{0.5} + C$$

Where Q_t is the adsorption capacity (mg/g) at time t (min), k_p is the diffusion rate constant (mg/g min^{1/2}) and C (mg/g) is a constant that gives an indication of the thickness of the boundary layer.

2.7 Tetracycline Desorption Experiments

Solution of Tetracycline (100.01 mL, 120 ppm) was mixed with 0.100 g of non- annealed composite material. The sample was equilibrated and shaken in the dark for 120 min at room temperature in neutral pH. After 120 min, the composite material was centrifuged and filtered from Tetracycline solution. The solid that separated was mixed with 20.01 mL DMSO in a water bath to extract adsorbed Tetracycline molecules from it.

2.8 Calibration Curve

UV-Vis Spectrophotometer was a fast, simple, and low cost convenient technique. It used to study the kinetic of concentrations of tetracycline

change. The absorbance of tetracycline was measured at 365 nm against a reagent blank prepared simultaneously.

Calibration curve is constructed by measuring the concentration and absorbance of several prepared solutions, called calibration standards. Once the curve has been plotted, the concentration of the unknown solution can be determined by placing it on the curve based on its absorbance or other observable variable. The calibration graphs of Tetracycline in different solvent are shown in Figures 3.1 and 3.2.

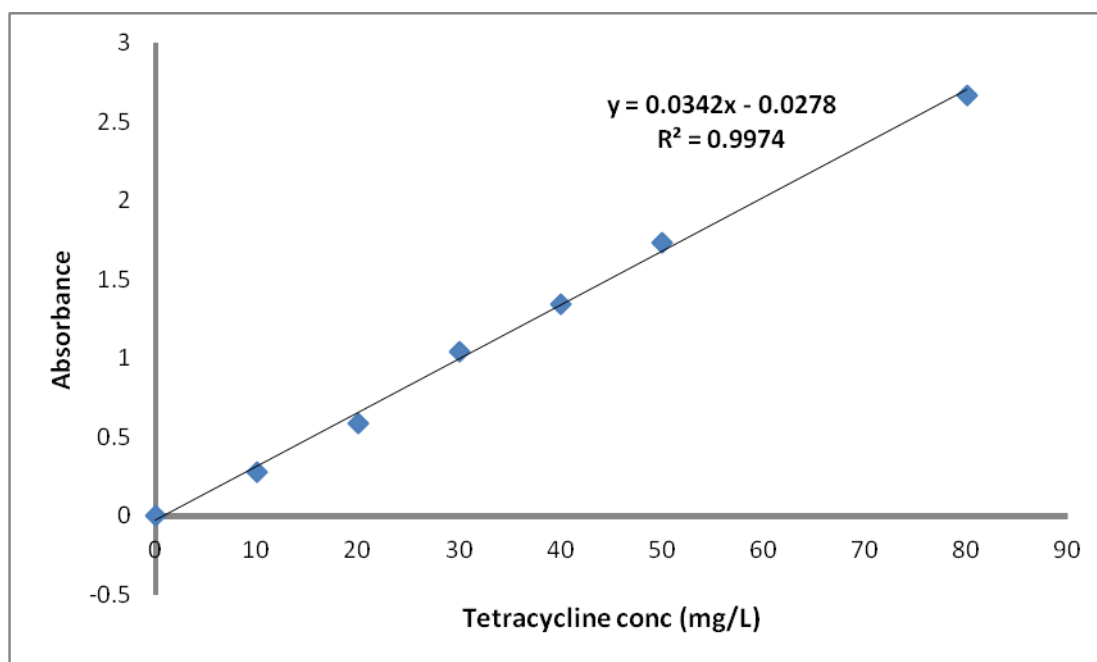


Figure 2.1: Atypical calibration curve for Tetracycline in Distilled Water by UV-Vis spectrometric method.

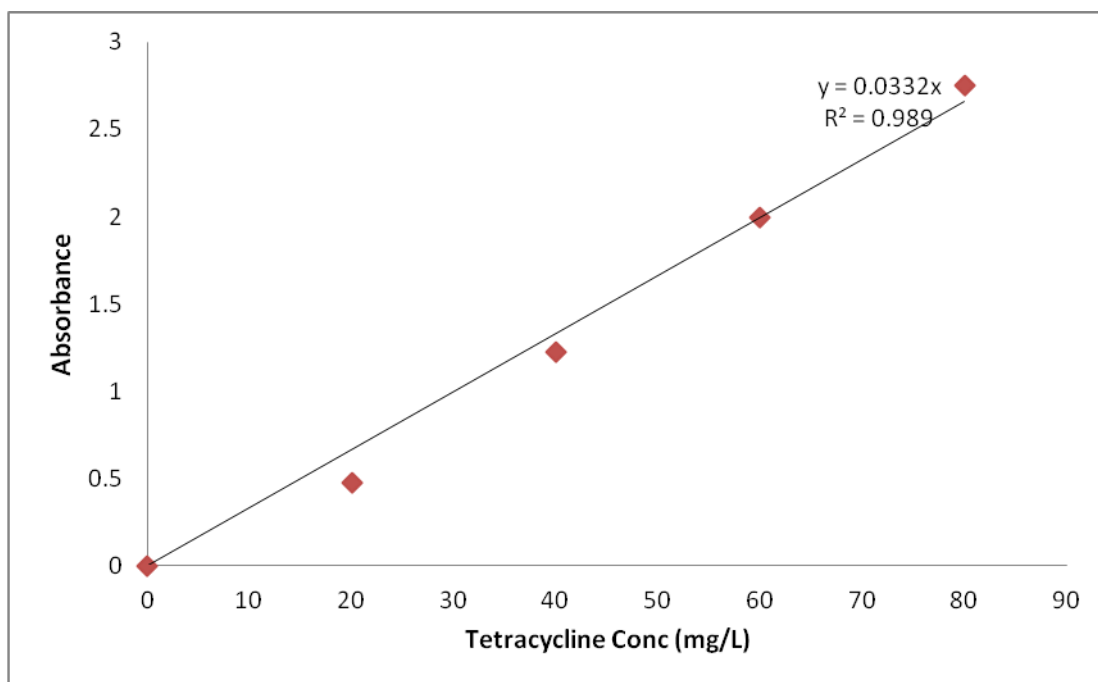


Figure 2.2: Atypical calibration curve for Tetracycline in DMSO by UV-Vis spectrometric method.

Chapter 3

Results and discussion

3.1 Catalysts Characterization

3.1.2 Photoluminescence (PL) Spectra of ZnO

Photoluminescence emission spectra were studied for commercial ZnO powder by dispersed small amount of ZnO powder in distilled water and placed in quartz cell, see Figure 3.1.

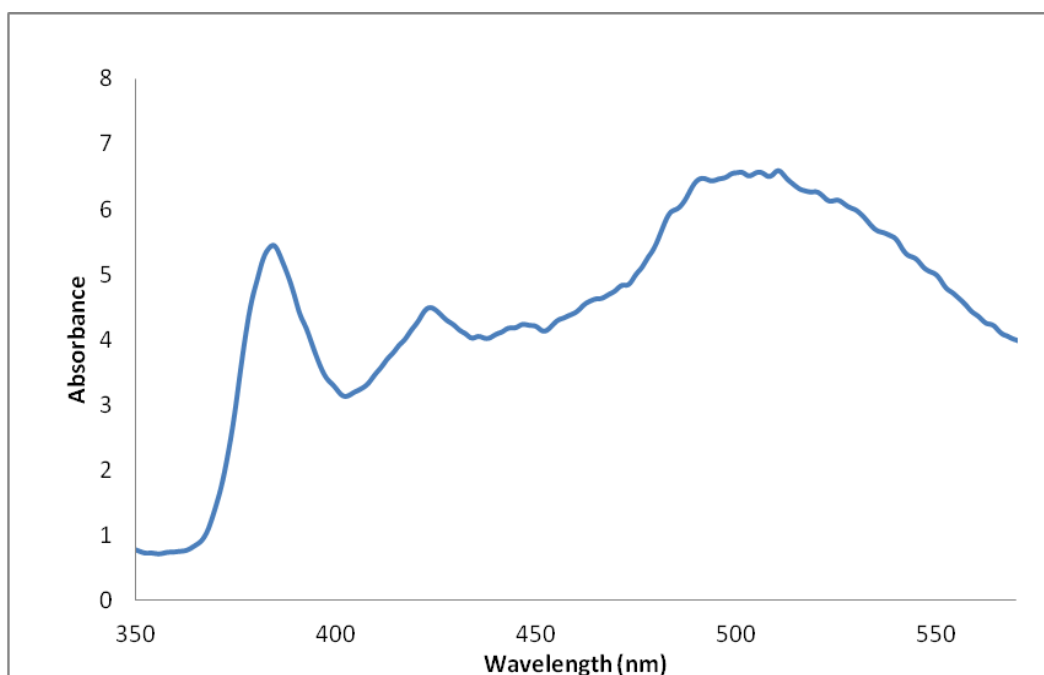


Figure 3.1: Photoluminescence spectra measured for commercial ZnO powder. (Baseline made on distilled water).

The observed emission peaks occurred at 385 nm and 425 nm in addition to a broad peak at 500 nm. At 385 nm, the intense emission peak shows that the band gap was 3.22 eV, consistent with reported value [73]. The band gap equivalent value was calculated from the relation $E_g \text{ (eV)} = 1240/\lambda_{\text{max}}$

(nm). The emission peaks at 425 nm are due to presence of oxygen vacancies [74].

3.1.2 Photoluminescence (PL) Spectra of Montmorillonite and Composite Material

The Photoluminescence plots of natural Montmorillonite aluminosilicate and ZnO/ Montmorillonite were measured as shown in Figure 3.2.

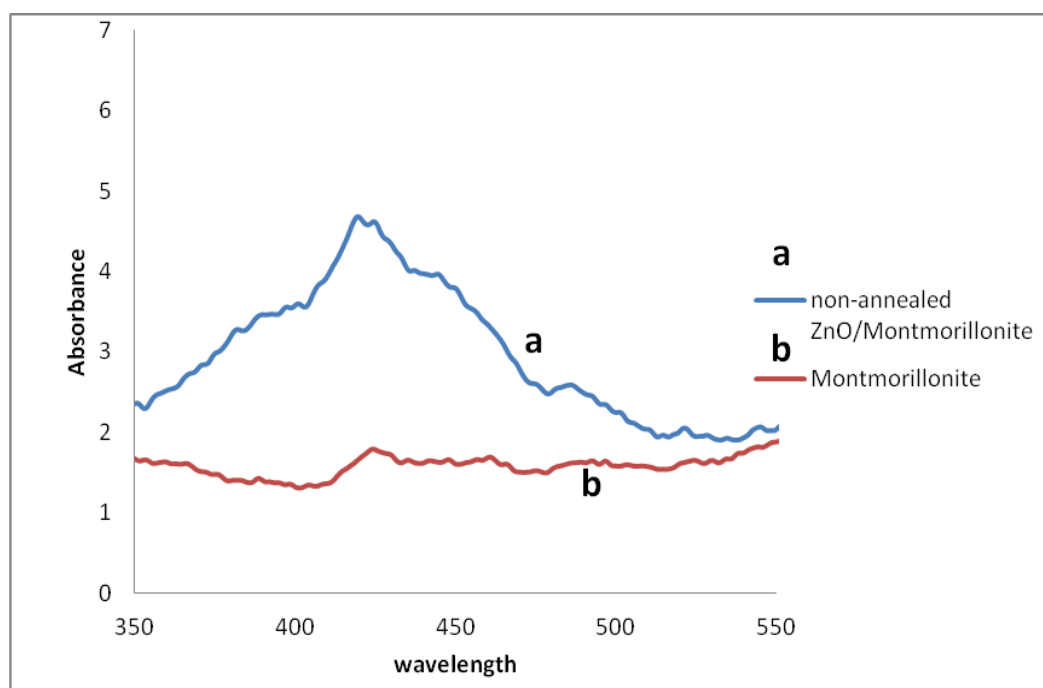


Figure 3.2: Photoluminescence of a) ZnO/ Montmorillonite and b) Montmorillonite clay minerals.

There is no significant peak for Montmorillonite in PL spectra; at 425 nm, there is a peak that may indicate the presence of oxygen vacancies. However, the peak at 385 nm in composite material appeared for ZnO as an indication that ZnO attached with Montmorillonite. In addition, there are clearly increasing in absorbance of significant peak at 425 nm in the

composite ZnO/Montmorillonite than naked Montmorillonite may due to increase in oxygen vacancies.

3.1.3 ZnO XRD Characterization

XRD pattern was measured for commercial ZnO and prepared nano-ZnO powder as shown in Figures (3.3, 3.4). The X-ray pattern showed a hexagonal wurtzite crystal type for ZnO particles [75].

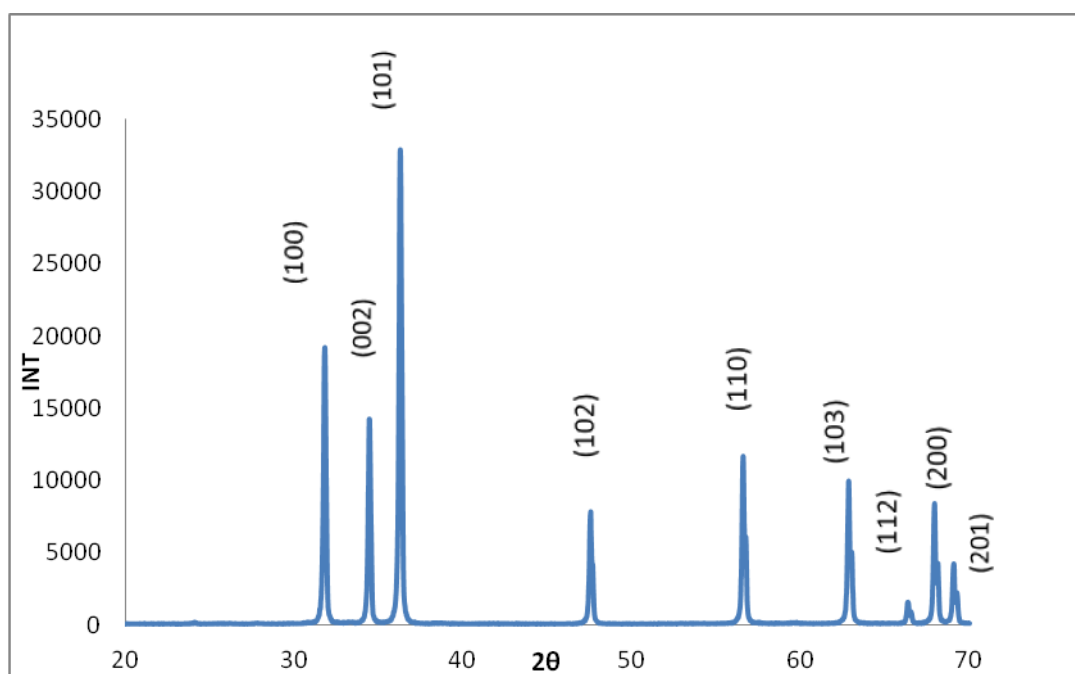


Figure 3.3: X-ray diffraction pattern for commercial ZnO powder.

The peaks positioned at diffraction angles (2θ) of 31.5° , 34° , 36° , 47.5° , 56° , 62.5° , 67.47° and 68.46° can be assigned to the reflections from (100), (002), (101), (102), (110), (103), (112) and (201) crystal planes, respectively, of a material with wurtzite-like structure [76].

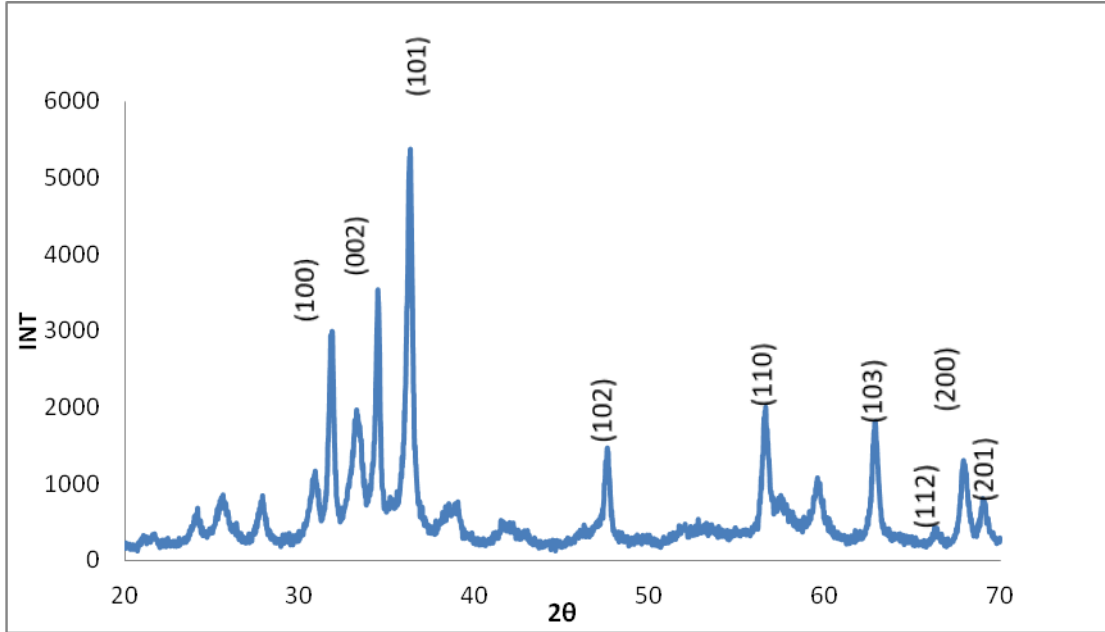


Figure 3.4: X-ray diffraction pattern for prepared ZnO powder.

Figure 3.4 shows XRD patterns for prepared ZnO powder. The two peaks at $2\theta = 31^\circ$ and 45.5° belong to NaCl impurity, as evidenced from literature [77]. The impurity peaks belong to NaCl, which may result during preparation reaction. The Scherrer equation [78] was used to calculate the ZnO particle diameter,

$$D = \frac{K \lambda}{\beta_{1/2} \cos\theta}$$

where β is the line broadening at half the maximum height in radians, K is the shape factor with a typical value of about 0.9, λ is the X-ray wavelength (0.15418 nm), θ is the Bragg angle and d is the mean size (averaged diameter of crystallites in nm) of the ordered (crystalline) domains angle. The Scherrer equation shows that the average particle size for the prepared nano- ZnO powder is 27 nm. The commercial powders showed 46 nm size.

3.1.4 XRD Pattern for Montmorillonite

XRD pattern of Montmorillonite was measured as shown in Figure 3.5. The Figure shows peaks at 20, 22, 36.3 and 62.4°. The distance between atomic layers in Montmorillonite was calculated by using Bragg's Law.

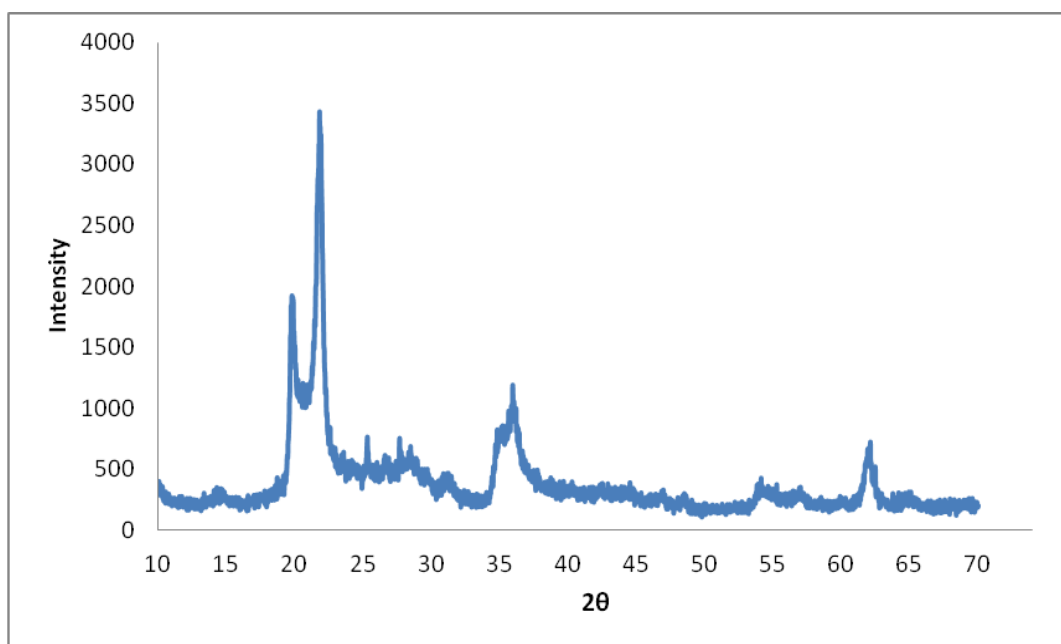


Figure 3.5: X-ray diffraction pattern for Montmorillonite.

Bragg's Law refers to the simple equation:

$$d = \frac{n \lambda}{2 \sin \theta}$$

The variable d is the inter planer distance in the crystal, θ is the Bragg angle and the variable λ is the wavelength of the incident X-ray beam and n is an integer. From the Figure 3.5, d is 0.45 nm ($n = 1$, $\lambda = 1.541 \text{ \AA}$).

3.1.5 XRD Pattern of ZnO/Montmorillonite

X-ray diffraction pattern for ZnO/Montmorillonite composite material was measured as shown in Figure 3.6.

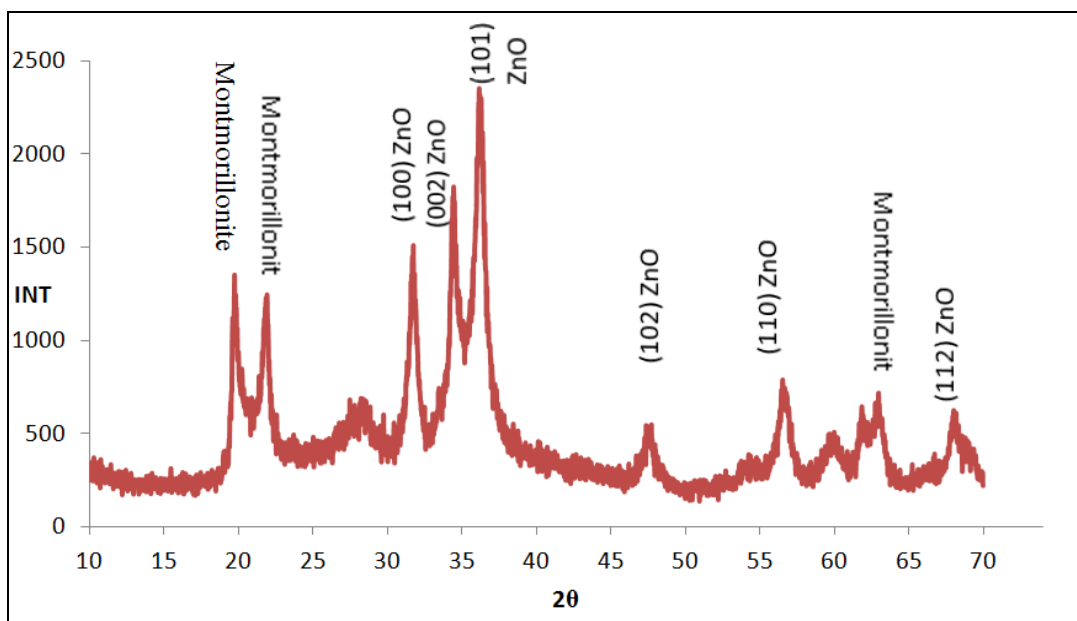


Figure 3.6: X-ray diffraction pattern for prepared ZnO/Montmorillonite composite material.

Most of ZnO peaks, as (100), (002) and (101), appeared in the pattern as a strong indication that the ZnO particles existed onto Montmorillonite surface through preparation step. By using Bragg's Law, interlayer distance (d) was calculated for Montmorillonite (0.45 nm). This is the same value for naked Montmorillonite, which means that ZnO particles do not enter between layers of Montmorillonite but only reside its surface. The peaks for Montmorillonite in the composite material appeared (at $2\theta = 19.8$ and 21.7) less sharp and more broadening than the one for naked Montmorillonite. This broadening may indicates that the Montmorillonite crystals have been distorted through the supporting process and this lead to increase the surface area of composite material also this explain why the

activity of adsorption increased when using composite material in this work.

X-ray pattern was measured also for air annealed and N₂ annealed ZnO/Montmorillonite composite material, as shown in Figures 3.7 and 3.8.

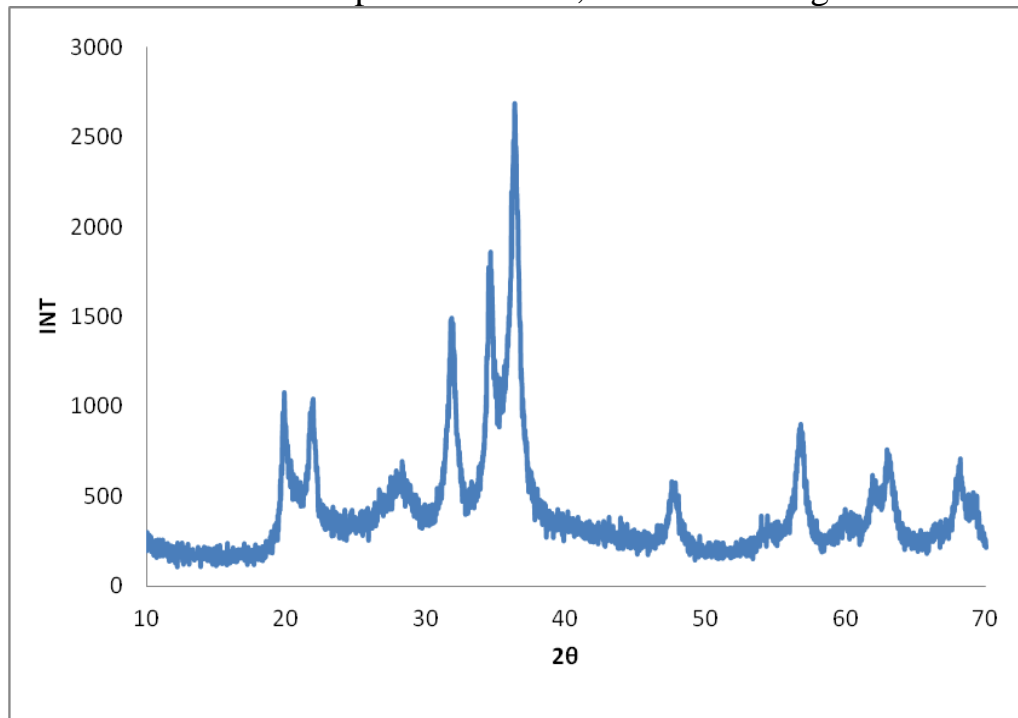


Figure 3.7: X-ray diffraction pattern for prepared N₂-annealed ZnO/Montmorillonite composite material.

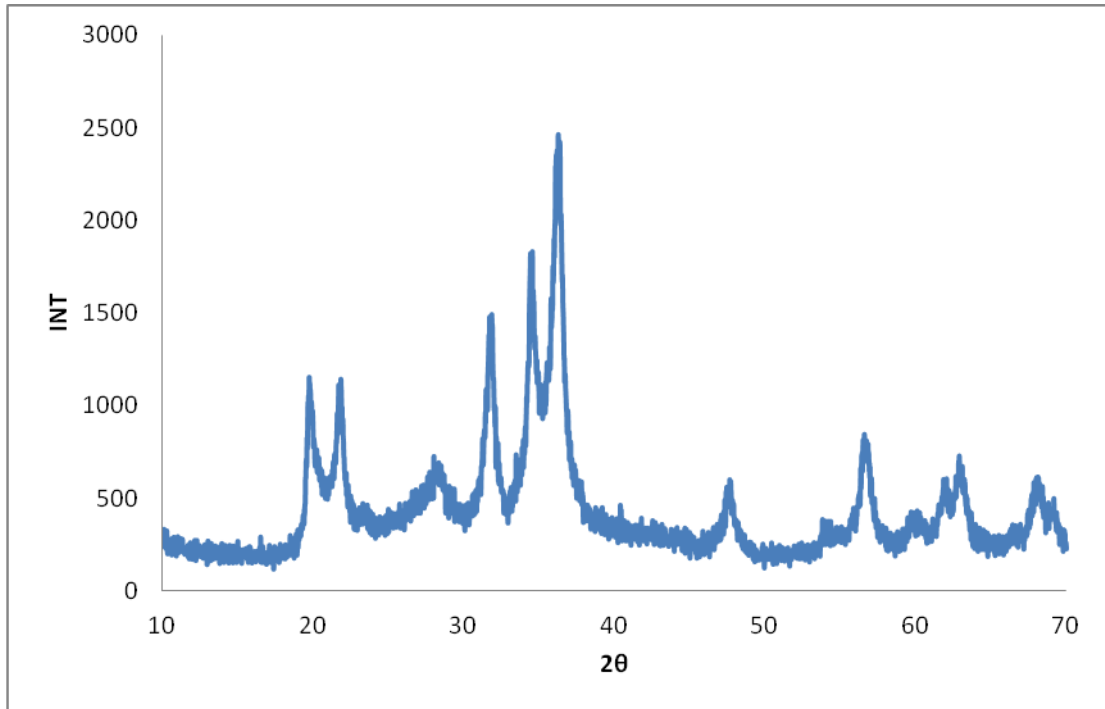


Figure 3.8: X-ray diffraction pattern for prepared air-annealed ZnO/Montmorillonite composite material.

There is no difference in X-ray patterns between the two types of annealed powders according to Figures 3.7 and 3.8. Moreover, annealing patterns did not have any significant differences comparing with non-annealed ZnO/Montmorillonite pattern. This means that the annealing process at 450°C does not affect or change the crystallites of the composite material. Montmorillonite is thermodynamically stable and need high temperature to melt (thermal effects occur at temperature $\geq 900^{\circ}\text{C}$, by the exclusion of some volatile components or changing the crystalline of it [79]).

3.2 Tetracycline Adsorption Experiments

3.2.1 Effect of Adsorbent Type

Values of percent Tetracycline removal on different prepared adsorbents are shown in Figure 3.9. The Figure shows that prepared ZnO/Montmorillonite has higher adsorption capacity than either annealed or non-annealed naked Montmorillonite.

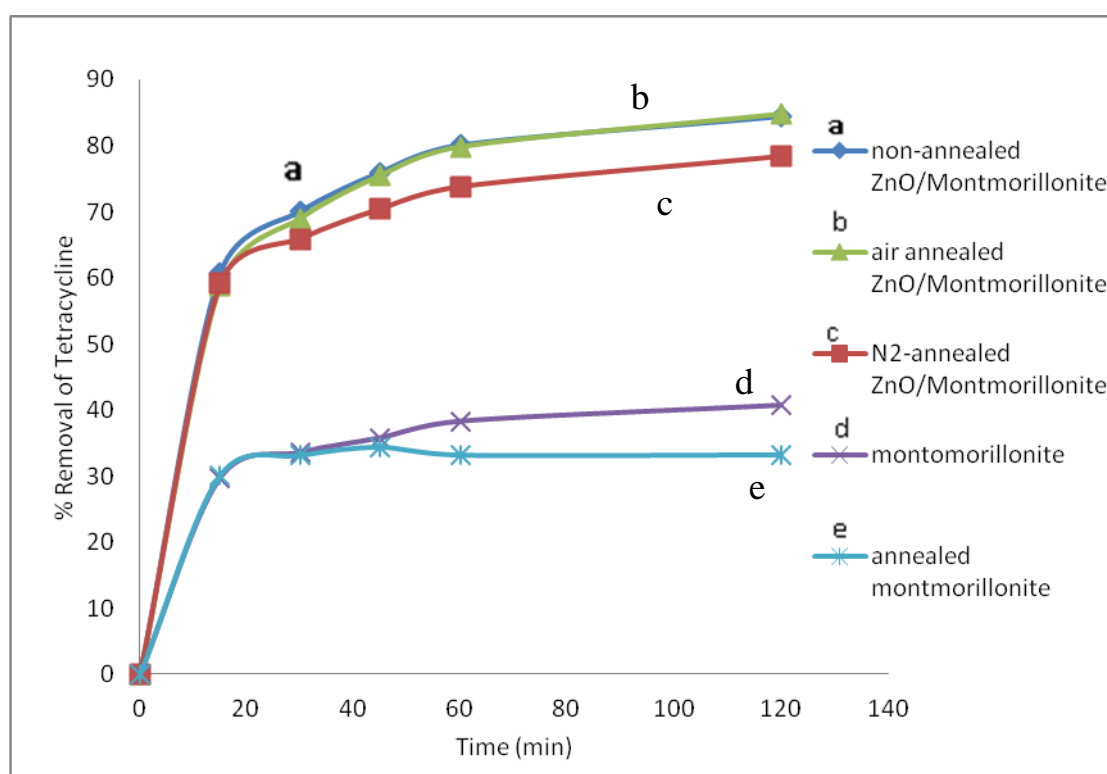


Figure 3.9: Percentage of Tetracycline removal by different types of adsorbent, a) non-annealed b) annealed with air c) annealed with N₂ d) Montmorillonite e) air- annealed Montmorillonite at (initial conc.:120 mg/L, temperature: 25 °C, 0.1g of adsorbent in a neutral medium).

The experimental results demonstrated that air-annealed ZnO/Montmorillonite, at 450°C, showed higher Tetracycline adsorption than the N₂-annealed adsorbent. However, in this work and according to

the XRD results (see Figures 3.9) annealing at 450°C did not affect the morphology of Composite material in both cases of annealing.

In the case of N₂-annealing, molecules of nitrogen gas expel oxygen (O₂) and oxides located on the surface of the adsorbent and force them to leave out from the sites and pores. Oxygen leaves as O₂ and its electrons go back to the metal ions (M²⁺) on the surface of solid. This may decrease the surface area and adsorption activity of solid. In case of annealing with air and non-annealing, the surface is rich with oxides in the cavity of Montmorillonite, which increases adsorption and enhances the penetration of Tetracycline into the adsorbent more than in N₂ annealing.

However, the non-annealed adsorbent showed similar adsorption capacities to air annealing adsorbent (no change in XRD patterns, see Figures 3.6-3.7). Therefore, there is no need to anneal the ZnO/Montmorillonite composite material if it is used in adsorption process. As shown in Figure 3.9 and Table 3.1, After 100 min, non-annealed ZnO/ Montmorillonite removed about 83 % of Tetracycline compared to ~ 40 % adsorption by commercial Montmorillonite. It has been found that the activity of composite form with ZnO increased by ~ two fold. During the supporting process, the size of Montmorillonite particles was supposed decrease with stirring and the surface area increased, see Figures 3.5 and 3.6, peaks at $2\theta = 21$ and 22° be less sharp in composite material than that for commercial Montmorillonite (Further study of surface area recommended)

Adsorption on Montmorillonite in neutral medium is due to intercalation of Tetracycline between layers, with reported distance of 14.7 Å [80]. Moreover, hydrogen bonding between polar Tetracycline groups and acidic groups on clay may also be involved [80].

Table 3.1: The percentage removal of Tetracycline by different types of adsorbent after 100 min adsorption.

| Type of Adsorbent | % Removal |
|---|-----------|
| ZnO/Montmorillonite (non-annealed) | 83 % |
| ZnO/Montmorillonite (annealed with air) | 83 % |
| ZnO/Montmorillonite (annealed with N ₂) | 74% |
| Montmorillonite | 40% |
| Annealed Montmorillonite | 30% |
| ZnO | 2 % |

The effect of adsorption time on Tetracycline removal was also studied for different types of adsorbent, as shown in Figure 3.9. Table 3.2 demonstrates the effect of adsorption time on the removal of Tetracycline using non-annealed ZnO/Montmorillonite. There is a gradual trend of increase in percentage removal of Tetracycline as adsorption time increased.

Table 3.2: The percentage removal of Tetracycline with time by using non- annealed ZnO/Montmorillonite for 60 min adsorption.

| Time (min) | % Removal of Tetracycline |
|------------|---------------------------|
| 0 | 0 |
| 15 | 61 |
| 30 | 70 |
| 45 | 76 |
| 60 | 80 |

3.2.2 Effect of Tetracycline Concentration

Adsorption of Tetracycline by adsorbents may depend on the initial concentration of Tetracycline. The adsorption of Tetracycline on non-annealed ZnO/Montmorillonite was investigated using different initial concentrations ranging from 60 ppm to 120 ppm.

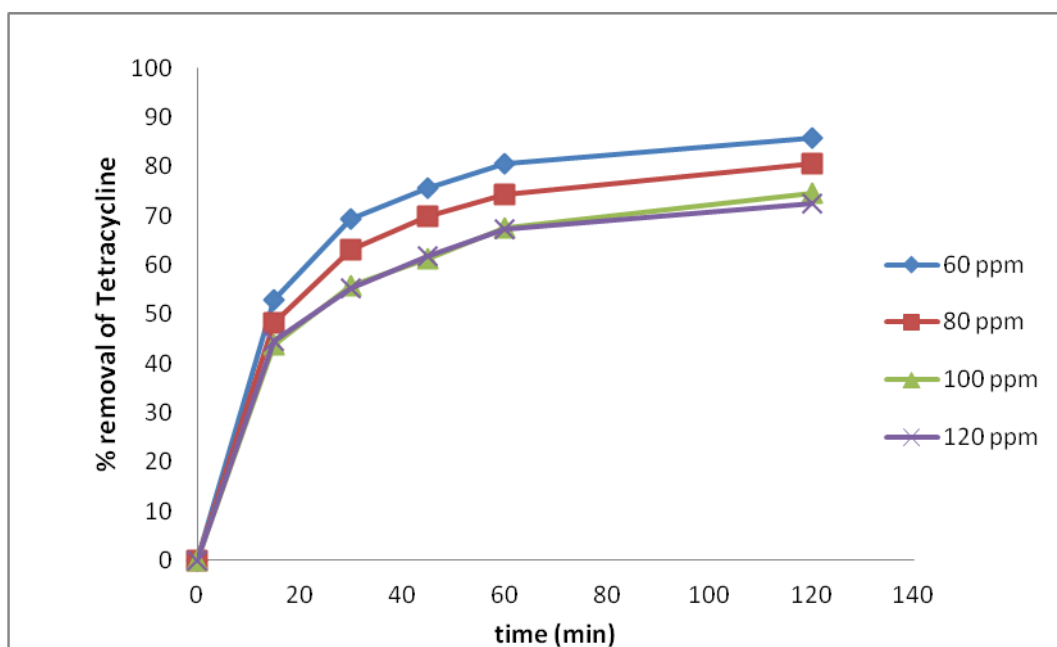


Figure 3.10: Effect of Tetracycline initial concentration on the adsorption process at (temperature: 25°C, amount of non-annealed ZnO/ Montmorillonite adsorbent 0.1 g at pH=7).

The results, Figure 3.10, show the percentage of removal decreases with increasing initial concentration. When changing the initial concentration of Tetracycline solution from 60 to 120 ppm, the amount adsorbed increased from ~ 51 ppm (85 % removal) to 84 ppm (70 % removal) at 25 °C after 120 min. Thus amount of adsorbed Tetracycline per gram adsorbent increased with increasing initial Tetracycline concentration, see Figure 3.11. This means that the adsorbent still has useful active sites after time pass.

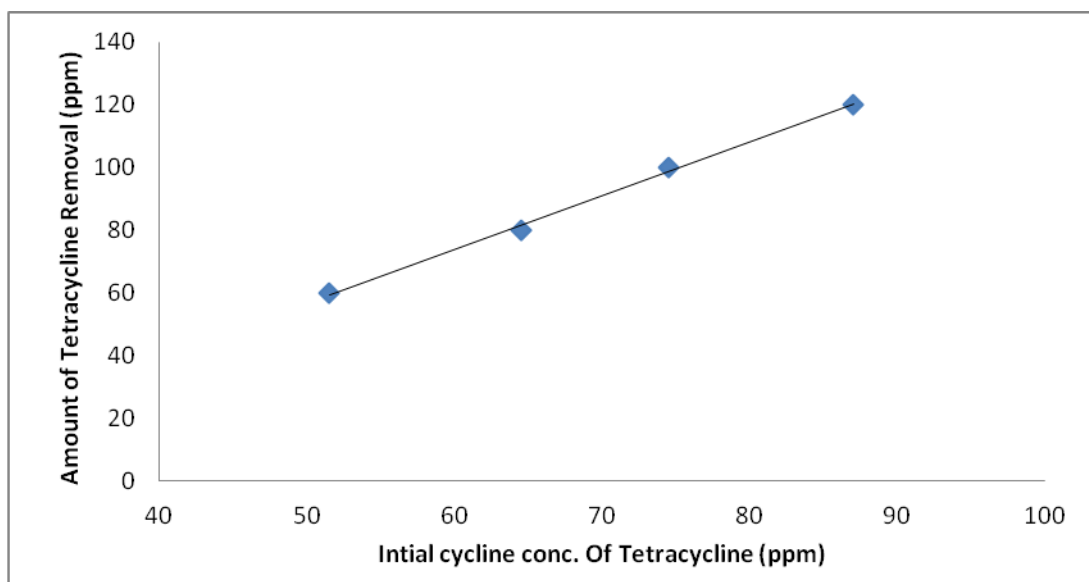


Figure 3.11: Amount of Tetracycline removal variation with changing initial concentration of Tetracycline after 120 min using (0.1 g non-annealed ZnO/ Montmorillonite adsorbent, temperature: 25°C and pH=7).

3.2.3 Effect of pH

Effect of solution pH on Tetracycline adsorption on non-annealed ZnO/Montmorillonite was investigated. Tetracycline molecule has three ionizable functional groups (Figure 3.12) [81]. The charge of the molecule depends on the pH of solution. The adsorption behavior may also depend

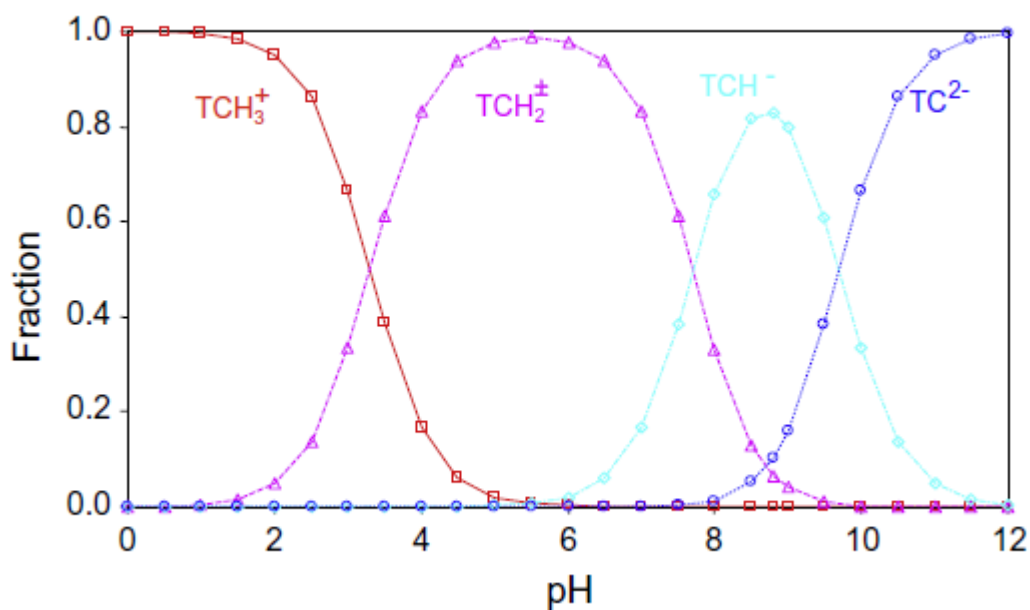


Figure 3.13: Speciation of Tetracycline under different pH values (TC: Tetracycline and TCH₃⁺ means protonated Tetracycline) [81].

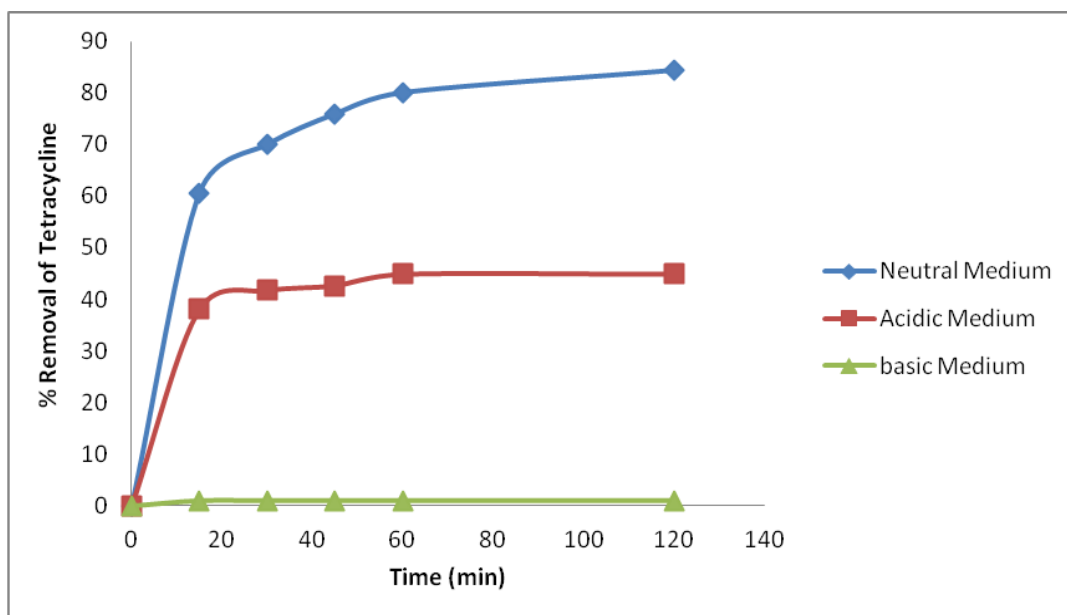


Figure 3.14: Effect of pH on Tetracycline removal by non-annealed ZnO/Montmorillonite adsorbent with contact time at (initial concentration 80 ppm, temperature 25°C and 0.1g ZnO/Montmorillonite adsorbent).

The highest percentage removal of Tetracycline occurred in the neutral medium, followed by acidic one, as shown in Figure 3.14. High adsorption onto composite materials was assumed to be caused by multiple

simultaneous interactions between charged functional group of Tetracycline and surface charge sites of Montmorillonite clay [25]. The cation-exchange mechanism between negatively charged clay surface and cations of Tetracycline was suggested to be dominant in acidic media [37].

High adsorption capacity in a neutral pH may be due to surface complexation mechanism between clay and Zwitter ions of Tetracycline, which was accompanied with proton uptake and favorable on acidic clay. In addition, physical mechanisms such as hydrogen bonding, van and der Waals forces and attraction between polar Tetracycline functional groups and acidic groups on the surface of Montmorillonite improve the adsorption of Tetracycline. No adsorption was observed under high pH (alkaline conditions) where repulsion mechanism might be involved between negative Montmorillonite surface and Tetracycline anionic form. Similar results have been found in earlier work when naked Montmorillonite was used for Tetracycline adsorption [83].

3.2.4 Effect of Temperature on Adsorption

The effect of temperature on the adsorption of Tetracycline onto non-annealed ZnO/Montmorillonite composite material has been investigated in the temperature range 25-75 °C. Figure 3.15 shows that the Tetracycline adsorption was not affected by the temperature. The slight deviation shown is an acceptable experimental error. Percentage of Tetracycline removal at different temperatures is ~ 75% after 100 min adsorption time. This is a good indication of the binding in the adsorption process.

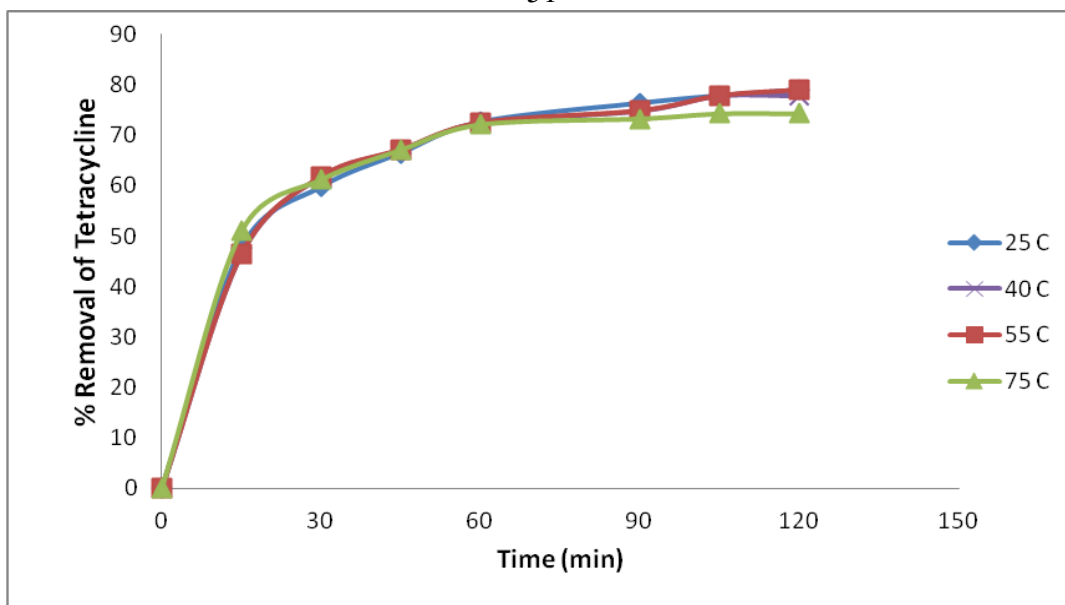


Figure 3.15: Effect of temperature on adsorption of 100 mL solution Tetracycline (120 ppm) using 0.10 g of non-annealed adsorbent at: a) 25°C b) 40°C c) 55°C d) 75°C. For better temperature control, adsorption process was conducted using thermostated water bath for 120 min at pH=7.

The results here indicate that the adsorption process is a physisorption with very small activation energy. Physical adsorption is a reversible process, where equilibrium is achieved rapidly and energy requirements are small. Chemical adsorption, involves stronger forces, is specific and thus requires larger activation energy [84]. Under neutral conditions, physisorption is presumably dominant, whereas under acidic conditions chemisorption (with ion exchange) may be dominant process.

3.2.5 Kinetics of Tetracycline Adsorption

The kinetics of Tetracycline adsorption on non-annealed ZnO/Montmorillonite were investigated. Equilibrium was reached in 120 min (Figure 3.16), compared to 60 min with Montmorillonite adsorbent.

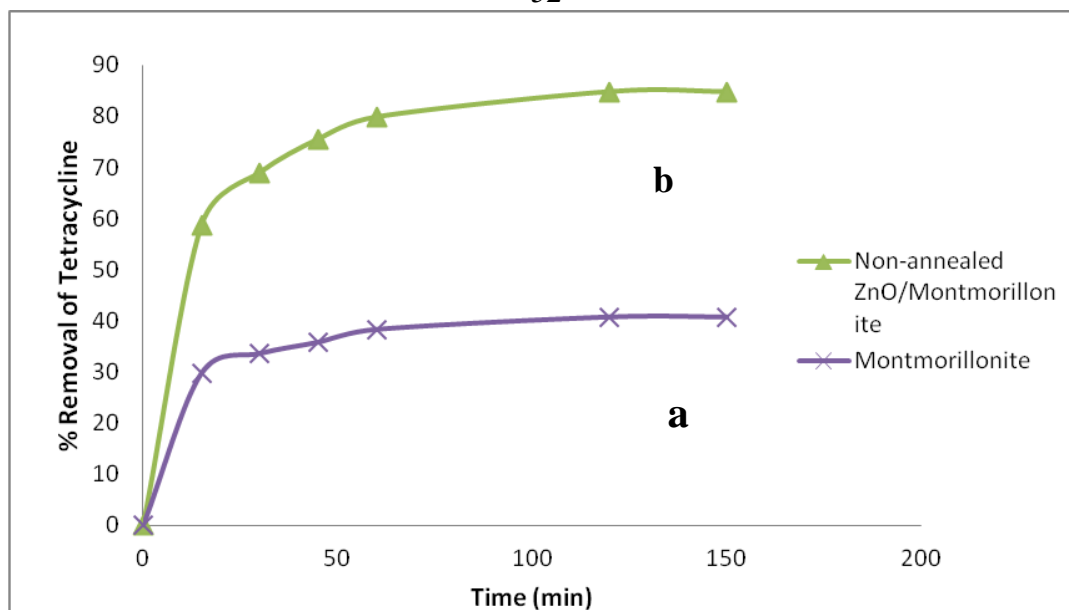


Figure 3.16: Percentage removal of Tetracycline by adsorption with a) Montmorillonite b) non-annealed ZnO/Montmorillonite at 0.1 g adsorbent, 120 ppm Tetracycline, pH=7 at room Temperature).

In order to investigate the mechanism of Tetracycline adsorption process on Montmorillonite and ZnO/ Montmorillonite adsorbent, the pseudo- first-order kinetic model, pseudo-second-order model and intra-particle diffusion model were applied and plotted to find the most applicable model. We plot $\log (q_e - q_t)$ versus t , and (t/q_t) versus t to check for the pseudo- first- order kinetic and pseudo-second-order models, respectively. The results are shown in Figures 3.17 – 3.18. For intra-particle diffusion model, q_t is plotted against $t^{1/2}$ to get a straight line, see Figure 3.19. (All mathematical terms were defined in section 2.6.8).

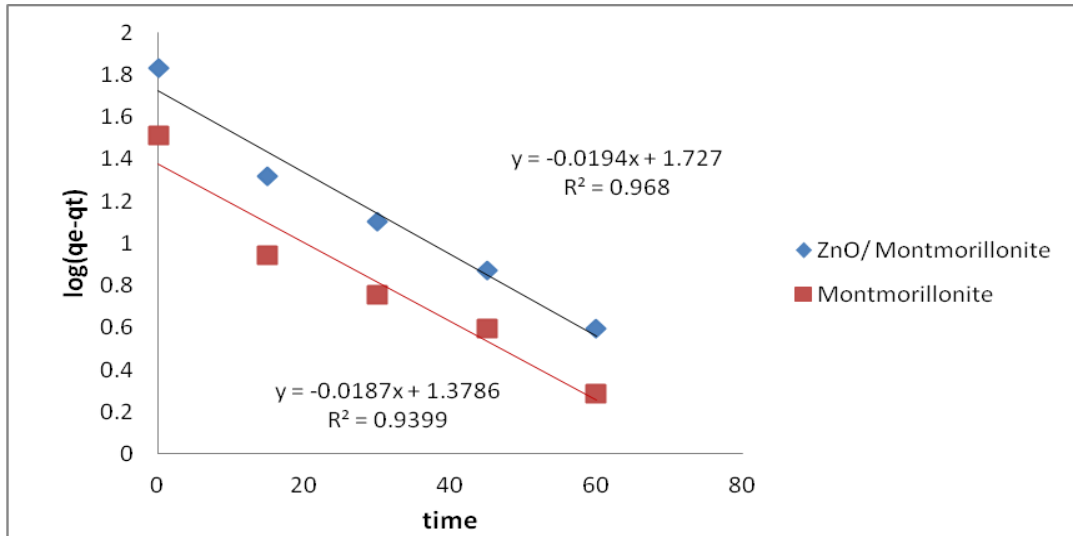


Figure 3.17: Kinetics of Tetracycline removal according to the pseudo-first-order model by non-annealed Montmorillonite/ZnO and nicked Montmorillonite at (initial concentration: 80 ppm, pH=7, temperature: 25 °C and 0.1g adsorbant).

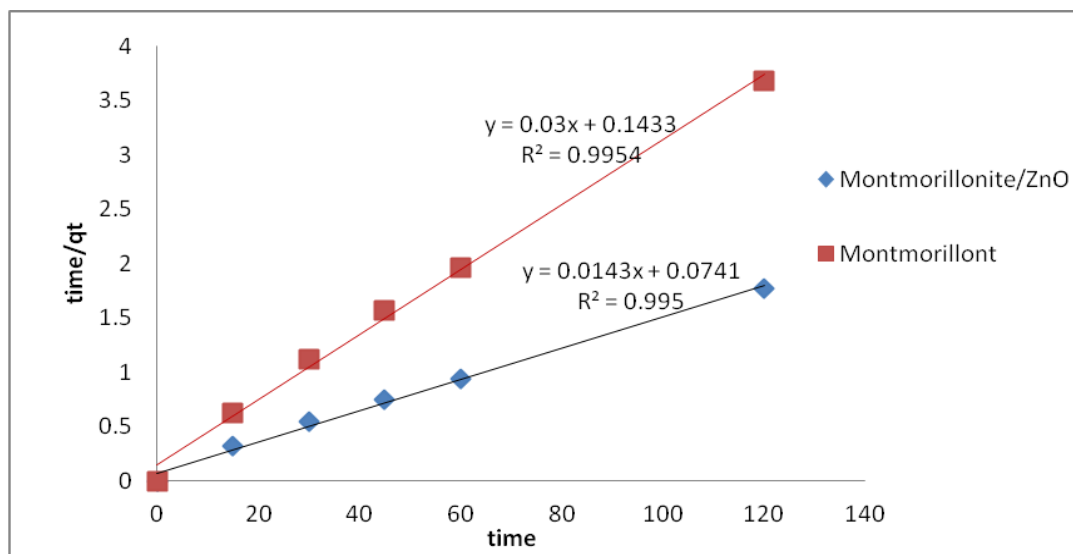


Figure 3.18: Kinetics of Tetracycline removal according to the pseudo-Second-order model by Montmorillonite/ZnO and nicked Montmorillonite at (initial concentration: 80 ppm, pH: 7, temperature: 25 °C and 0.1 g adsorbent).

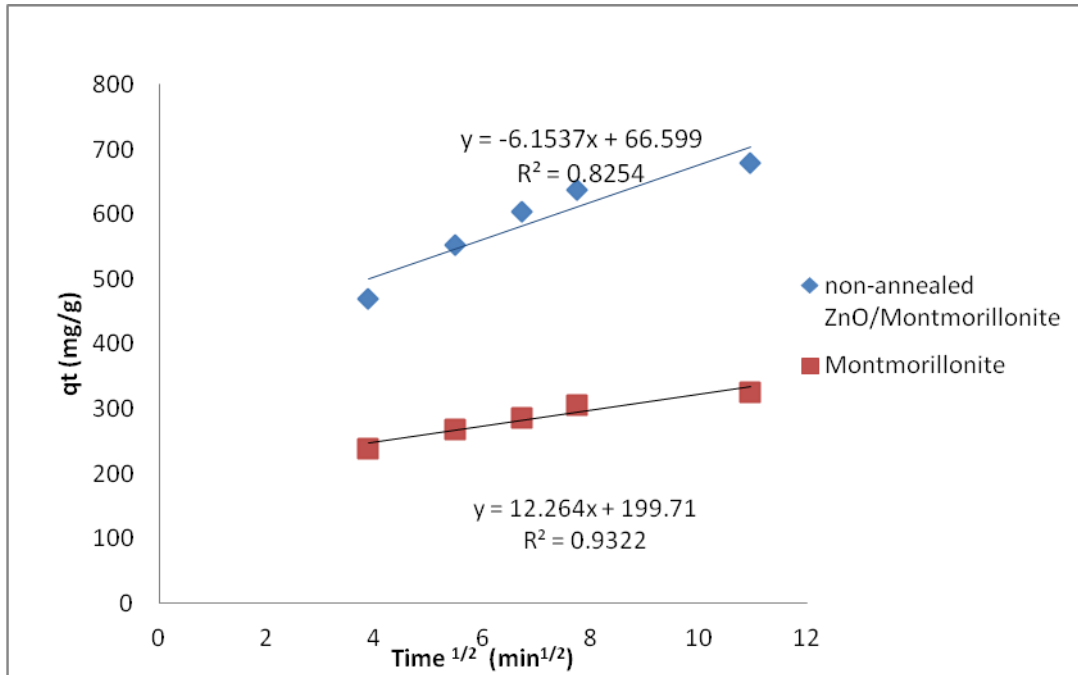


Figure 3.19: Kinetics of Tetracycline removal according to the intra-particle diffusion model by Montmorillonite/ZnO and nicked Montmorillonite at (initial concentration: 80ppm, temperature: 25 °C and 0.1g adsorbent).

Value of k_1 and q_e were calculated using the slope and intercept of plots of $\log (q_e - q_t)$ versus t (Figure 3.17, Table 3.3). Table 3.3 shows the correlation coefficients and other parameters calculated for pseudo- first-order kinetic and pseudo-second-order kinetic models.

Table 3.3: The correlation coefficients and other parameters measured for pseudo- first- order kinetic and pseudo-second-order kinetic models.

| Adsorbent | q_e (exp) (mg/g) | pseudo- first- order kinetic model | | | pseudo-second-order models | | |
|---------------------|-----------------------|--|------------------------|-------|--------------------------------------|------------------------|-------|
| | | K_1 (min^{-1}) (10^{-2}) | q_e (calc) (mg/g) | R^2 | K_2 (g/mg min) (10^{-3}) | q_e (calc) (mg/g) | R^2 |
| Montmorillonite | 40 | 4.307 | 23.911 | 0.94 | 6.28 | 33.33 | 0.99 |
| ZnO/Montmorillonite | 85 | 4.468 | 53.333 | 0.97 | 2.76 | 69.93 | 0.99 |

Table 3.3 shows the parameters for There are good agreement between pseudo second-order kinetics parameters and experimentally observed equilibrium adsorption capacity (q_e), in addition to relatively higher R^2 values than those for the pseudo first order model. This indicates that Tetracycline adsorption onto Montmorillonite followed pseudo second-order kinetics. In case of ZnO/Montmorillonite adsorbent, $q_{e(\text{exp})}$ values for reaction are more closer to calculated ones obtained from pseudo second-order kinetics.

Table 3.4 summarizes correlation coefficients and parameters for Tetracycline adsorption onto Montmorillonite and ZnO/ Montmorillonite according to intra-particle diffusion kinetic model. In Figure 3.19, straight line does not pass through the origin, which indicates that mass transfer limits the adsorption rate across the boundary later.

Table 3.4: Intra-particle diffusion model parameters for Tetracycline adsorption onto Montmorillonite and ZnO/ Montmorillonite at 25°C.

| Adsorbent | K (mg/g min^{1/2}) | C | R² |
|-----------------------------|---------------------------------------|----------|----------------------|
| Montmorillonite | 12.2 | 199.7 | 0.93 |
| ZnO/ Montmorillonite | -6.15 | 66.6 | 0.83 |

Pseudo second-order kinetics is more suitable to describe the kinetics. It assumes that the rate-limiting step may be chemisorption involving valency forces through exchange or sharing of electrons between adsorbent and adsorbate [85].

3.2.6 Adsorption Isotherms

Adsorption systems are usually described by isotherms, which give some important information about adsorption process such as adsorption capacity [86]. The adsorption isotherm for Tetracycline onto non-annealed ZnO/Montmorillonite at 25°C is shown in Figure 3.20. The effect of isotherm shape can be used to predict if an adsorption is a favorable process.

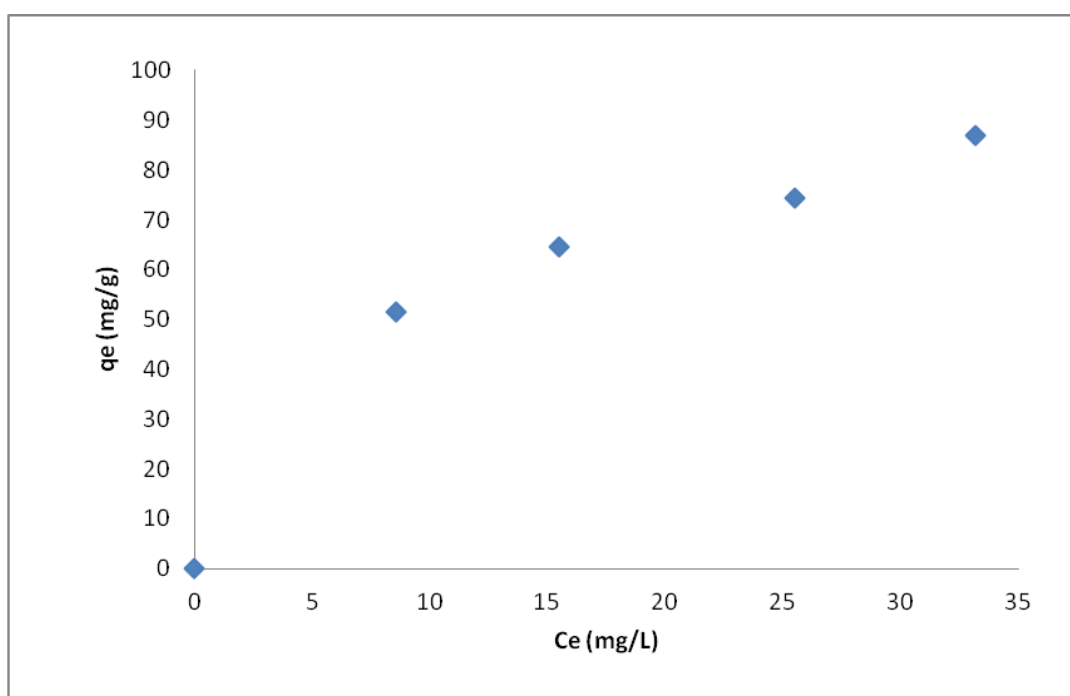


Figure 3.20: Equilibrium adsorption isotherm of Tetracycline onto non-annealed ZnO/Montmorillonite adsorbent at 25°C and neutral medium.

Adsorption of Tetracycline by non-annealed ZnO/ Montmorillonite was modeled using both Freundlich and Langmuir isotherms with the quality of the fit assessed using the correlation coefficient. Determination of Freundlich isotherm constants K_f and n from the intercept and slope of a plot of $\log q_e$ versus $\log C_e$, see Figure 4.21. In Figure 3.22, Langmuir

adsorption isotherm was investigated by plotting C_e/q_e versus C_e , where the slope and intercept were used to calculate Q_0 and b (All mathematical terms defined in section 2.6.7).

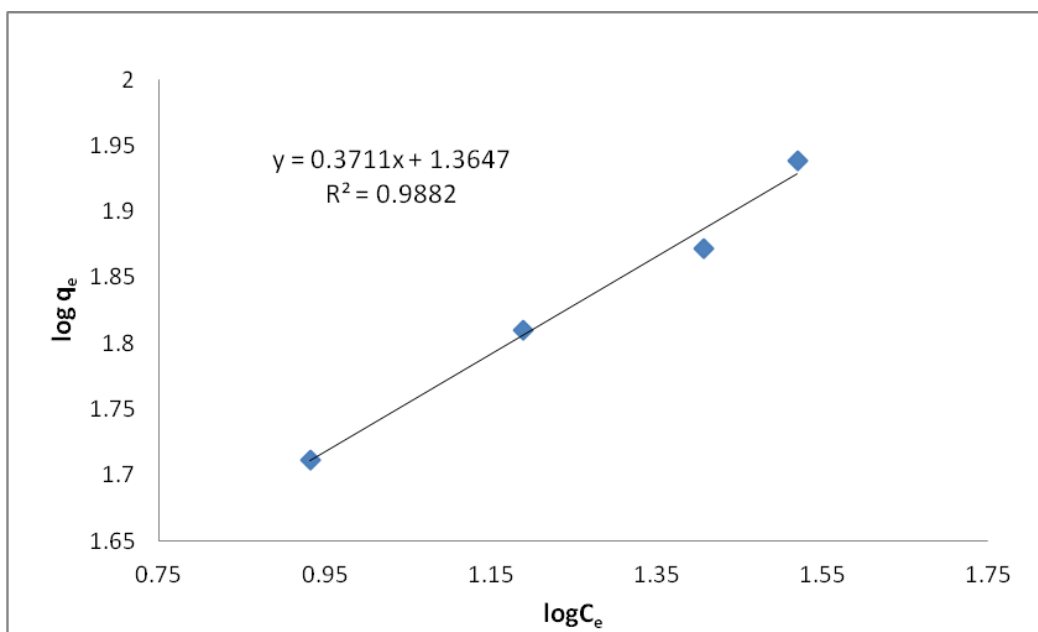


Figure 3.21: Freundlich plot for Tetracycline adsorption onto non-annealed adsorbent at 25°C and neutral medium.

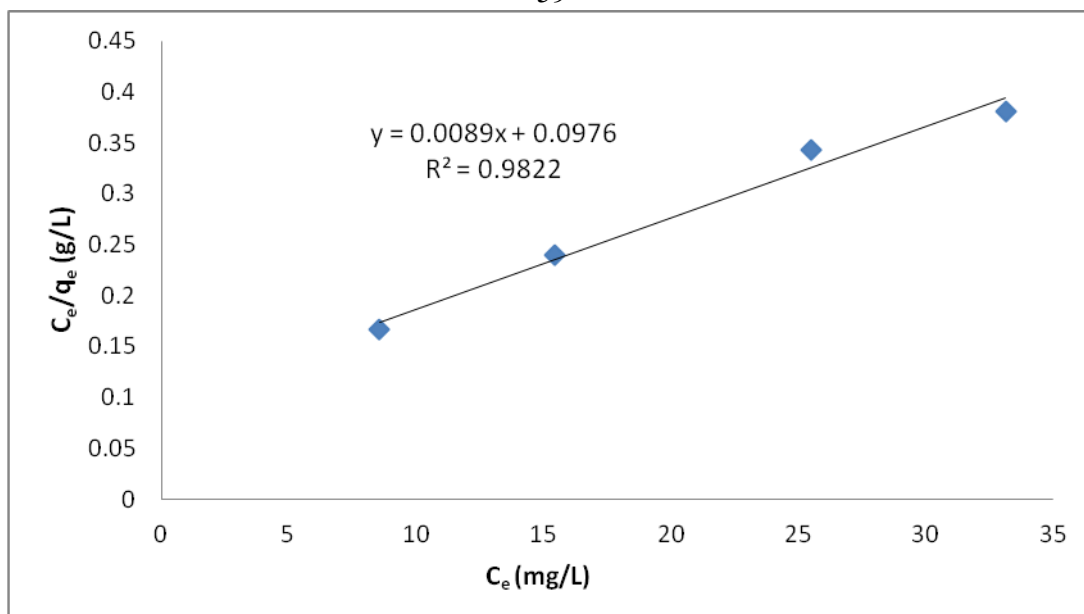


Figure 3.22: Langmuir plot for Tetracycline adsorption onto not annealed adsorbent at 25°C and neutral medium.

Table 3.5 summarizes simple adsorption isotherm model parameters that are most frequently applied. The term n is the Freundlich constant and k_F is the Freundlich adsorption constant. The r^2 was 0.9882 and 0.9822 when the data were fitted to the Freundlich and Langmuir models, respectively. The Freundlich model provided a slightly better fit to the observed data while the Langmuir model could provide adsorption capacity that might be used to describe the adsorption process. In the current study, Langmuir model can describe adsorption process and it was described the adsorption onto naked Montmorillonite in previous study [80]. The adsorption capacity was 112.36 mg/g.

Table 3.5: Adsorption isotherm models coefficients for Tetracycline adsorption.

| Isotherm | Langmuir Model constant | | | Freundlich Model Constant | | |
|--------------|--------------------------|-------------|----------------|--|--------|----------------|
| | Q _o (mg/g) | b (L/mg) | R ² | k _f ((mg/g)(L/mg) ^{1/n}) | n | R ² |
| Tetracycline | 112.36 | 0.0912 | 0.9822 | 23.158 | 2.6947 | 0.9882 |

The Langmuir isotherm assumes that [87]:

- The surface of the adsorbant strongly attracts dissolved adsorbate molecules on its surface.
- The surface has a specific number of sites where the adjacent solute molecules can be adsorbed.
- No interaction occurs between adsorbate molecules.
- Only one layer of molecules adsorb onto the surface (monolayer adsorption).

3.3 Tetracycline Photo- Degradation Studies

The photo-catalytic degradation activities were studied for Tetracycline solution. For solar light irradiation, the photo-catalyst was placed in a beaker containing 100 ml of Tetracycline solution. Then, the beaker was placed under solar simulated lamp with $19.0337 \times 10^{-5} \text{ W/cm}^2$ intensity, which was stacked onto a magnetic stirrer for 75 min. The distance between the photo-catalyst system and the light source was fixed at 70 cm.

The experiment was repeated with changing different variables as Tetracycline concentration, pH and contact time. Blank experiments were done without the presence of photo-catalysts in the Tetracycline solution.

Figure 3.23 shows that the absorbance spectra of the Tetracycline solution have two peaks at approximately 272 and 356 nm. The maximum absorption wavelength that was chosen for measurement was 356nm [88].

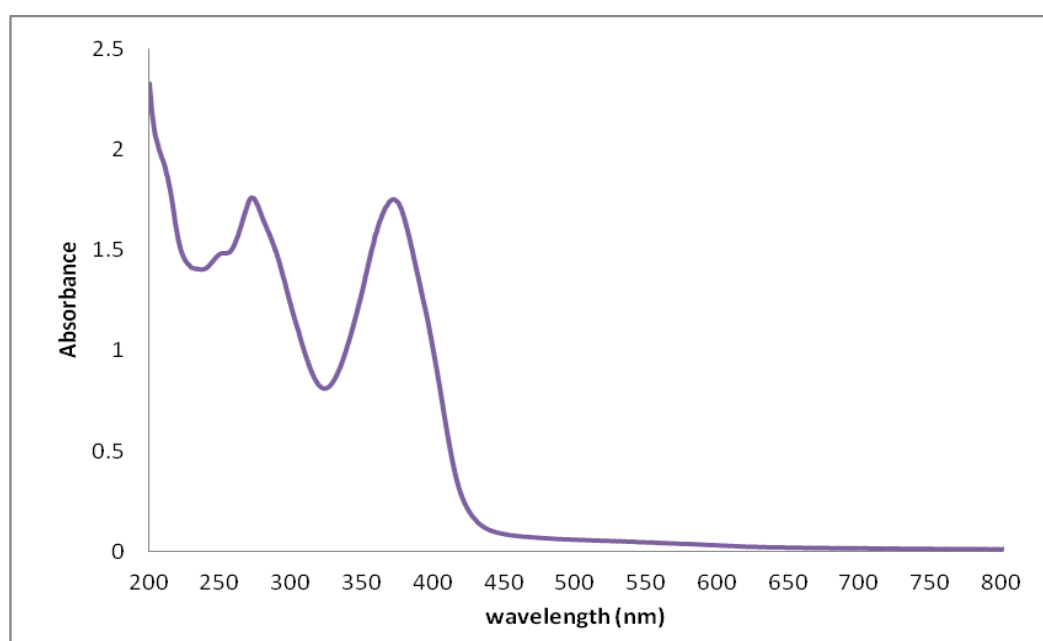


Figure 3.23: Absorption spectra of Tetracycline solution in distilled water in a neutral pH at room temperature.

Figure 3.24 shows the decrease in absorbance intensity at 365 nm of the Tetracycline in the presence of photo-catalyst. After 60 min of radiation, the peak dramatically disappeared compared with the initial concentration. This is due to photolytic reaction of Tetracycline induced by the absorption of UV light in the presence of photo-catalyst ZnO, which leads to the degradation of Tetracycline. ZnO demands UV region for excitation, due to its band gap (3.2 eV), and has limited photo-catalytic applications to

shorter wavelengths only [89]. However, UV light is expensive; so it is more suitable to use solar light, which is non-costly. Solar light involves ~ 5% UV only; it is thus required to investigate efficiency of ZnO systems under solar light.

After 15 min, a new peak at 520 nm appeared, which is due to an intermediate product from Tetracycline photo-degradation in solution under simulated solar light. This new peak decreased with time of photolysis and disappeared after 1 hour, indicating complete degradation.

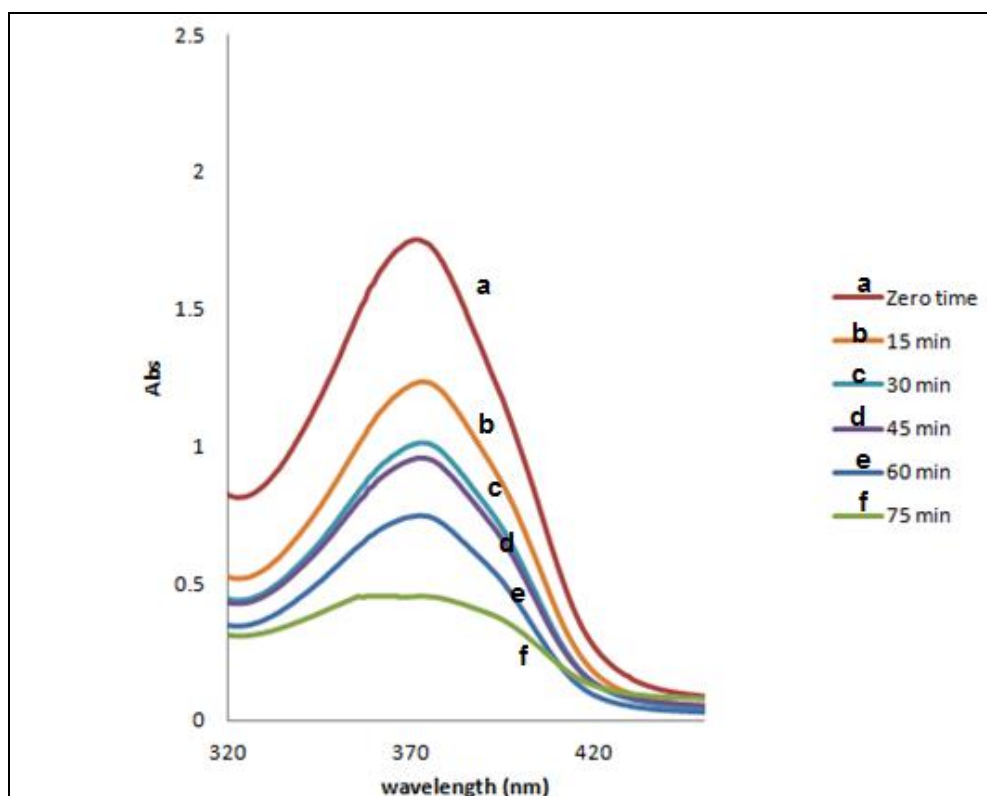


Figure 3.24: Spectro-photometric spectra of the photo-degradation of Tetracycline in the presence of ZnO photo-catalyst. Here, Absorbance of peak at 365 nm disappeared completely after 75 min at: 40 ppm Tetracycline, 0.1 g ZnO, room temperature and neutral pH medium under simulated solar light.

The direct photolysis of the Tetracycline in aqueous solution (40 ppm) without photo-catalyst can be ignored since no discoloration and degradation was observed after 60 min irradiation with simulated solar light. No significant adsorption was observed either.

Effect of adding photo-catalyst to contaminant solutions in the absence of light was studied. In the case of ZnO catalyst, Tetracycline concentration decreased only slightly (~ 2 ppm) until it reached a value after 30 min. When ZnO/Montmorillonite was used, relatively high loss of contaminant concentration occurred in the dark due to adsorption. Such observations were taken into consideration when studying the catalytic photo-degradation of Tetracycline.

3.3.1 Commercial ZnO Catalyst System

Commercial ZnO systems were used to catalyze photo-degradation of Tetracycline in water using simulated solar light.

3.3.1.1 Effect of ZnO Catalyst Amount

For commercial ZnO particle powder, Figure (3.25) shows that the Tetracycline degradation slightly increased with increasing pristine ZnO amount. However, at higher concentrations of ZnO the rate of photo-degradation was unchanged. This is due to screening effect by ZnO particles causing reduction in light penetration inside solution causing lowering in relative catalyst efficiency.

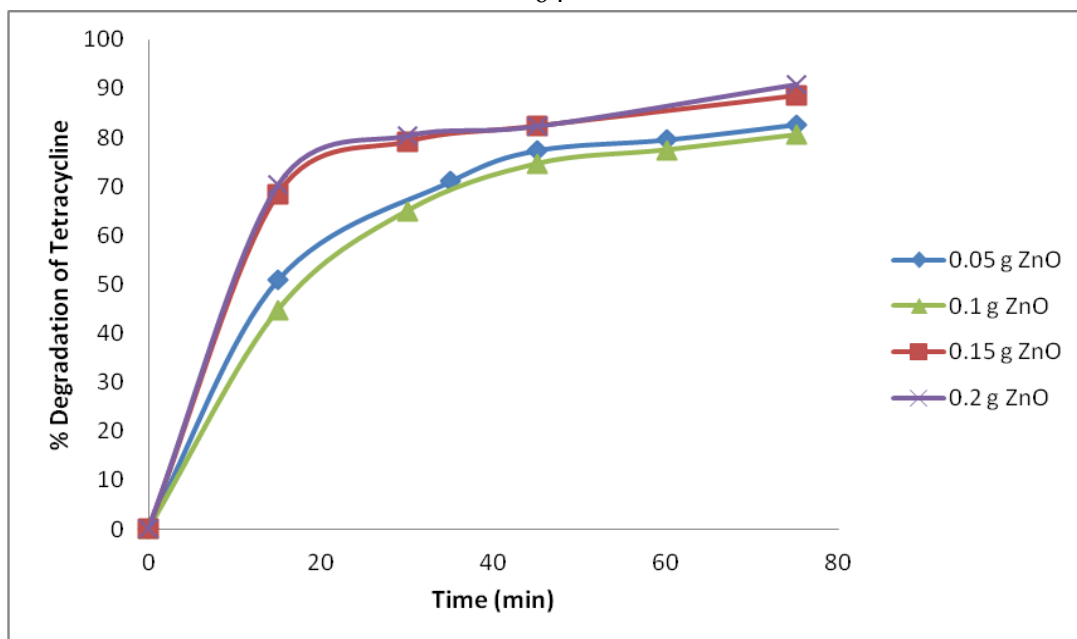


Figure 3.25: Effect of ZnO catalyst amount on degradation of Tetracycline at: solution concentration: 40 ppm Tetracycline, temperature: 25°C and neutral pH medium under simulated solar light.

The percentage of degradation, turnover frequency (TF), turnover number (TN) and quantum yield (QY) values were calculated after 15 min from each experiment. In the heterogeneous photo-catalysis reaction, the turnover number is the gross number of photo-generated transformations with respect to the number of active sites of the ZnO catalyst that is known.

$$TN = \frac{\text{no. of moles of reacted contaminant}}{\text{no. of moles of catalyst}}$$

Turnover frequency (TF) is the number of photo-catalytic turnovers per catalytic site and per unit time.

$$TF = \frac{TN}{\text{Time (min)}}$$

Quantum yield is defined as the amount (mol) of product formed or reactant consumed per photon of incident light at a given wavelength [90]:

$$Q.Y = \frac{\text{number of reacted molecules}}{\text{number of incident photons}}$$

$E (J) = \text{Incident power per unit area} \times \text{Total area or incident power} \times$
 $\text{Exposure time in second}$

$$= [(0.0001903 \text{ W/cm}^2) \times 21.6 \text{ cm}^2] \times [15 \times 60 \text{ second}] = 3.7 \text{ J}$$

Assuming average wavelength of incident light is 550 nm, then:

$$\nu = \frac{c}{\lambda} = \frac{3 \times 10^8 \text{ m s}^{-1}}{550 \times 10^{-9} \text{ m}} = 5.454 \times 10^{14} \text{ s}^{-1}$$

$E (J) = nh\nu$ Planks equation

$$n = \frac{J}{h\nu} = \frac{3.7}{6.62 \times 10^{-34} \times 5.454 \times 10^{14}} = 1.0244 \times 10^{19} \text{ photons}$$

From Table (3.6) and Figure 3.25, the TF and TN of Tetracycline degradation under simulated solar light decrease with increasing of ZnO amount. The initial rate of degradation increased by increasing the amount of catalyst, hence availability of more active sites on catalyst surface, will increase the rate. However, the relative efficiency of the catalyst decreases with increasing its amount. Increasing catalyst loading increased reaction rate up to a limited value. This is because when the amount of catalyst is

increased, the catalyst molecules may screen the radiation and prevent it from reach catalyst sites inside the reaction solution.

Table 3.6: Values of percentage of degradation, turnover number (TN), turnover frequency (TF) and quantum yield (QY) measured for Tetracycline degradation by changing ZnO amount after 15 min.

| Sample (g ZnO) | Initial rate | Turnover Number (TN) $\times 10^{-3}$ | Turnover Frequency (TF) (min^{-1}) $\times 10^{-4}$ | Q.Y (molecule/photon) |
|----------------|--------------|---------------------------------------|--|-----------------------|
| 0.05 | 0.03 | 7.46 | 4.97 | 0.27 |
| 0.1 | 0.03 | 3.30 | 2.20 | 0.24 |
| 0.15 | 0.04 | 3.34 | 2.23 | 0.36 |
| 0.2 | 0.05 | 2.57 | 1.72 | 0.37 |

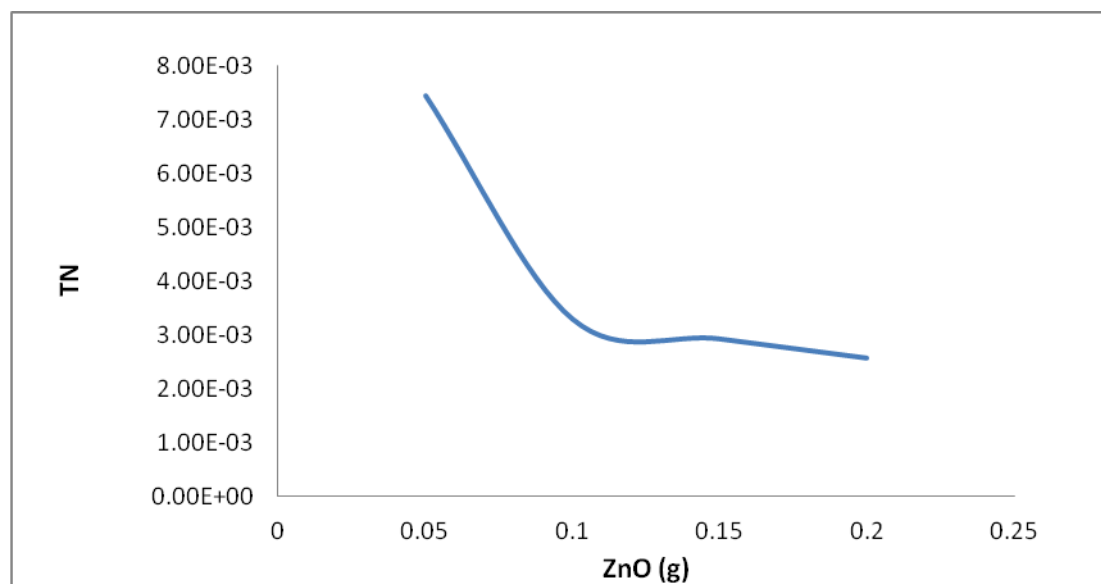


Figure 3.26: Effect of ZnO catalyst amount on Turnover number of Tetracycline degradation, at: solution concentration: 40 ppm Tetracycline, temperature: 25°C, 0.1 g ZnO and neutral pH medium under simulated solar light.

3.3.1.2 Effect of Tetracycline Concentration

Effect of initial Tetracycline concentration on initial rate of photo-degradation was studied under simulated solar light. The initial Tetracycline concentration was ranged from 10 ppm to 40 ppm, with constant catalyst loading 0.10 g in a 100 ml solution.

The initial rate of degradation was increased with increasing contaminant concentration as shown in Figure (3.27) and Table 3.7. Turnover number and quantum yield values calculated after 30 minutes for different concentrations of Tetracycline (10, 20, 30, and 40 ppm) are described in Table 3.7. The increasing T.N. and Q.Y. values indicate that the rate of photo-degradation increases by increasing the contaminant concentration.

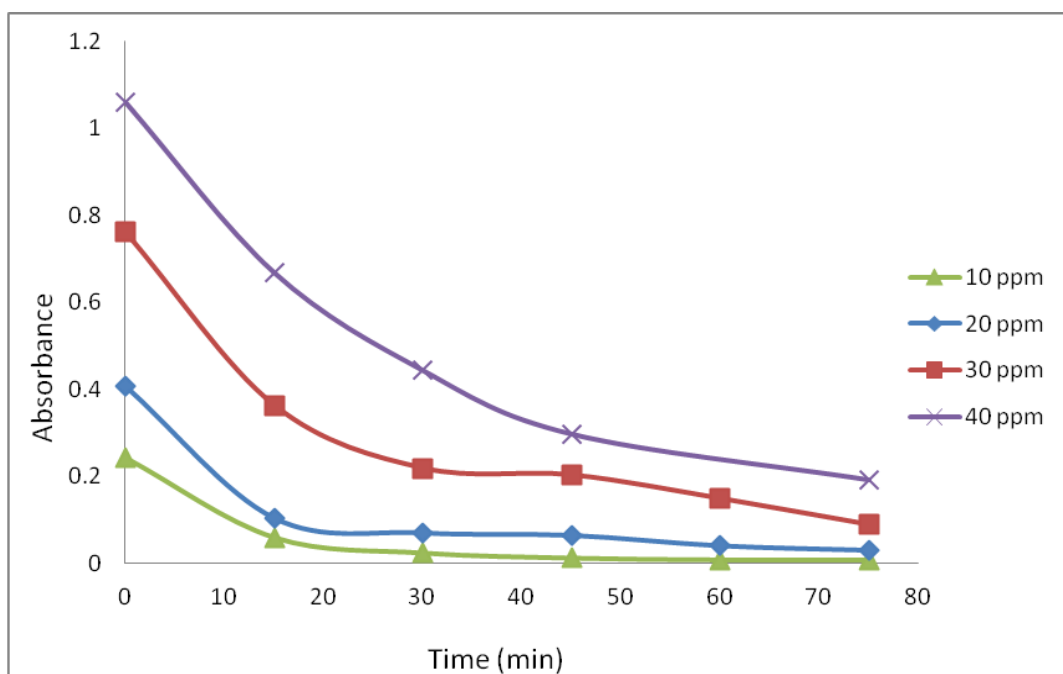


Figure 3.27: Effect of Tetracycline concentration on photo-degradation reaction: a) 10 ppm b) 20 ppm c) 30 ppm d) 40 ppm. By using 0.10 g ZnO in 100 mL solution and neutral pH at room temperature under direct solar light.

Table 3.7: Values of % degradation, turnover number (TN), turnover frequency (TF) and quantum yield (QY) measured for Tetracycline degradation after 15 min using different Tetracycline concentration

| Initial Tetracycline Concentration (mg/L) | % Degradation | Initial rate | Turnover Number (TN) $\times 10^{-3}$ | Turnover Frequency (TF) (min^{-1}) $\times 10^{-4}$ | Q.Y molecule /photon |
|---|---------------|--------------|---------------------------------------|--|----------------------|
| 10 | 72 | 0.012 | 1.32 | 0.88 | 0.10 |
| 20 | 75 | 0.020 | 2.75 | 1.83 | 0.20 |
| 30 | 56 | 0.026 | 3.06 | 2.04 | 0.22 |
| 40 | 45.5 | 0.026 | 3.11 | 2.08 | 0.24 |

Figure 3.27 shows that when the Tetracycline concentration was increased, the initial rate, QY and TF of degradation increased. The amount of Tetracycline that has been removed increased with increasing initial Tetracycline concentration. The plateau in Figure 3.28, slightly increasing in TN, is may due to light scattering effect [91]. When more Tetracycline amount is used, the Tetracycline molecules screen the radiation and prevent it from reaching catalyst surface inside the reaction mixture. This may stabilize the initial reaction rate after 40 ppm. Also in a photo-degradation mechanism, Active sites available on the surface of ZnO for HO \cdot generation will decrease because of adsorption competition between H $_2$ O/OH $^-$ and the Tetracycline molecules, and hence, the rate constant of degradation decreased in higher concentrations.

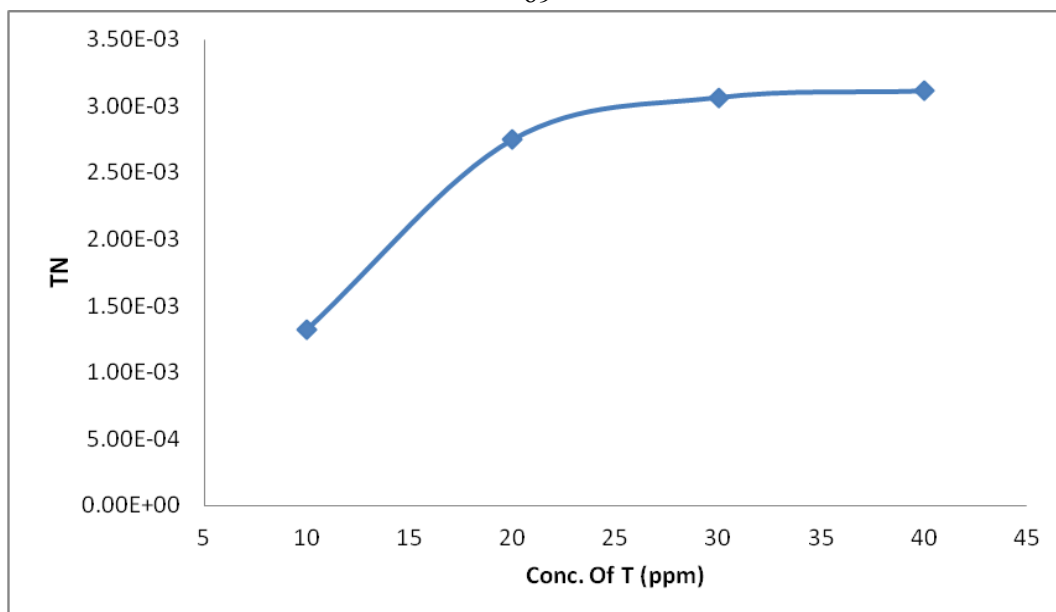


Figure 3.28: Effect of Tetracycline Concentration on Turnover number of degradation at catalyst amount: 0.1g, contact time: 15 min, pH = 7 and temperature: 25°C under simulated solar light.

3.3.1.3 Effect of pH on Photo-degradation of Tetracycline

According to previous studies, pH has a critical role in the photo-degradation process of many pollutants. When commercial ZnO powder was used for photo-degradation, the percentage of Tetracycline degradation increased basic > neutral >>> acidic medium. Figure 3.29 shows photo-degradation efficiency increased with higher pH.

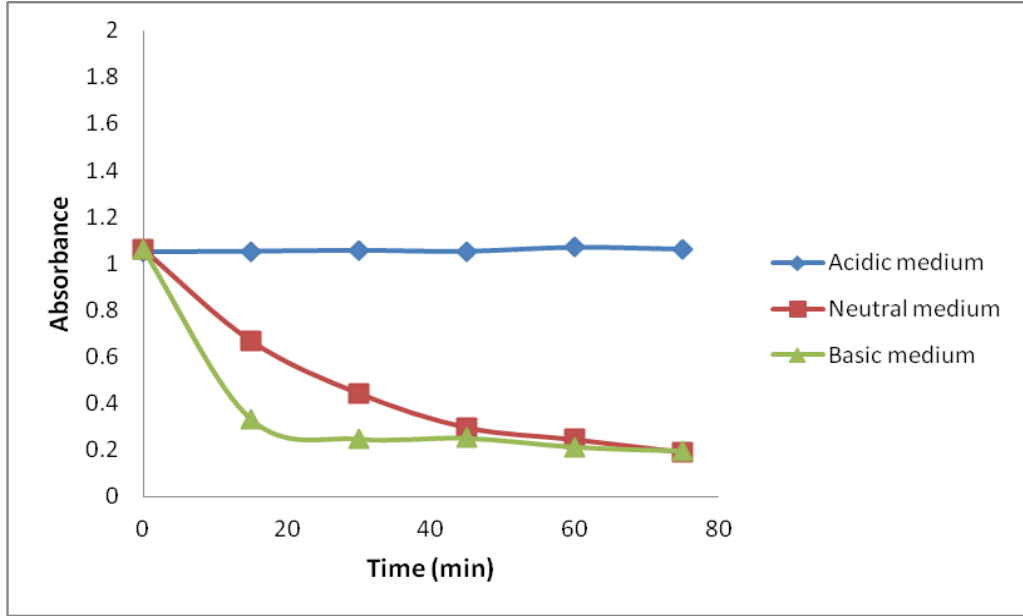


Figure 3.29: Effect of pH on degradation of Tetracycline with using (commercial ZnO powder catalyst amount: 0.1 g, Tetracycline concentration: 40 ppm, and temperature: 25°C under simulated solar light).

Table 3.8 shows that in the basic medium, the maximum photo-degradation efficiency is higher. Same results were reported for other processes [92]. Values of T.N and Q.Y also indicate same behavior. A possible explanation for this behavior is that there is a high concentration of adsorbed hydroxide anion (HO^-) in basic medium which encourage the hydroxide radical formation (Eq. (1.8)). The Tetracycline oxidation is then enhanced.



In a neutral solution, the reaction rates and the turnover number values are higher than in acidic solutions. As a result of amphoteric properties, ZnO can undergo photo-corrosion and dissociation under acidic conditions (Eq. (1.3)). The results do not encourage using ZnO in acidic media. Similar results have been reported in previous works with ZnO [92].

Table 3.8: Values of % degradation, turnover number (TN), turnover frequency (TF) and quantum yield (QY) measured for Tetracycline degradation after 15 min at different pH mediums.

| Sample | Degradation % | Initial Rate | TN (10^{-3}) | TF (min^{-1}) (10^{-5}) | Q.Y (molecule/photon) |
|----------------|----------------------|---------------------|----------------------------------|---|------------------------------|
| Acidic | 7.5 | 0 | 0.55 | 4 | 0.002 |
| Neutral | 45.5 | 0.03 | 3.11 | 20 | 0.010 |
| Basic | 69.5 | 0.05 | 5.09 | 34 | 0.017 |

The size of the particles and the distribution of the charges on the surfaces of the ZnO particles are also affected by the pH of the medium. In addition, the distribution of the particles of the photo-catalyst in the medium and the adsorption of Tetracycline on the surface of the photo-catalyst will also be affected by the pH [93].

3.3.1.4 Effect of ZnO Catalyst Type

Two types of ZnO powder were used, a commercial and prepared powders, in degradation of Tetracycline (see Figure 3.30).

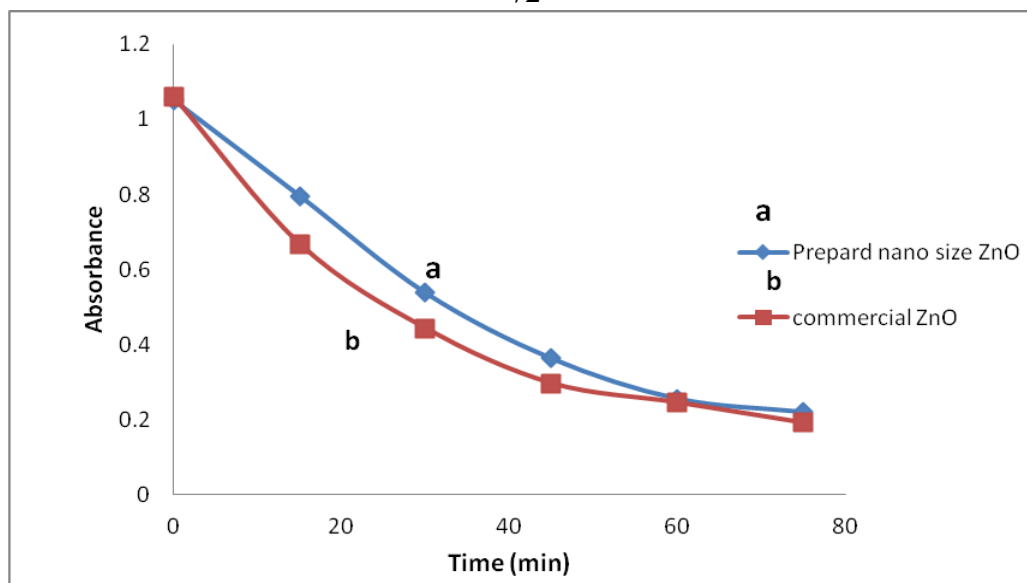


Figure 3.30: Effect of ZnO types with time on degradation of Tetracycline at (catalyst amount: 0.1g, Tetracycline concentration: 40 ppm, pH=7 and temperature: 25°C under simulated solar light).

Commercial Zinc oxide (46 nm) was found to be slightly more effective in degrading Tetracycline in aqueous solution than the prepared ZnO (27 nm). On using commercial ZnO in a solution of 40 ppm Tetracycline, the concentration of Tetracycline has decreased to 27 ppm after a period of 15 min (see Table 3.9). When the catalyst particle size decreases to less nano-size, its band gap increases, so relatively high energy is necessary to eject the electron from valance to conduction band. In this case, a lower wavelength needs to initiate the photo-degradation. Then prepared ZnO will work at lower wavelengths closer to UV-region. Therefore, the commercial powder will have more capability to absorb in the wavelength range closer to visible light (longer wavelength) than prepared ZnO.

Table 3.9: Values of percentage degradation, turnover number (TN), turnover frequency (TF) and quantum yield (QY) measured for Tetracycline degradation after 15 min using different ZnO type.

| Catalyst Type | Degradation % | T.N (10^{-3}) | T.F (min^{-1}) (10^{-5}) | Q.Y |
|----------------|---------------|-------------------|---|------|
| prepared-ZnO | 24.7 | 1.40 | 9 | 0.10 |
| Commercial ZnO | 37.8 | 2.38 | 16 | 0.17 |

3.3.2 ZnO/Montmorillonite Photo-Catalysis System

Figure 3.31 shows reaction profiles for using ZnO/Montmorillonite composite material as adsorbent and photo-catalyst for Tetracycline degradation.

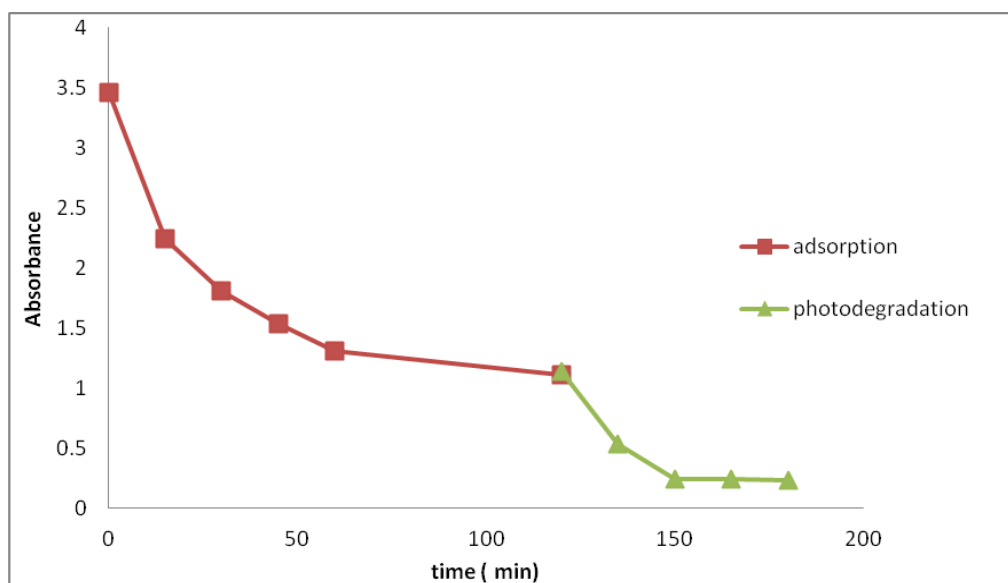


Figure 3.31: Adsorption and photo-degradation of Tetracycline by using non-annealed ZnO/Montmorillonite composite material at (catalyst amount: 0.1g, initial Tetracycline concentration: 100 ppm, pH=7 and temperature: 25°C under simulated solar light).

Solution of 100 ppm Tetracycline with 0.1 g non-annealed ZnO/Montmorillonite adsorbent was mixed and left at room temperature for 2 hours adsorption in dark, then the system was placed under direct solar light for one-hour. Adsorption process removed ~ 69 % from Tetracycline after equilibrium, then photo-degradation removed ~ 81 % (from remaining 31 % in solution). Around 94 % from the total Tetracycline concentration was successfully removed by dual effect. To be sure that all molecules adsorbed on the surface of composite material were degraded by light, Dimethyl sulfoxide (DMSO) was used to extract any adsorbed Tetracycline molecules from adsorbent before and after photo-degradation in two parallel experiments. After one hour of photo-degradation, 78% from the adsorbed Tetracycline molecules were completely photo-degraded. This mean that the supported photo-catalyst degraded a total of 94% of original Tetracycline. All in all, photo-degradation process seems to involve adsorption followed by total degradation.

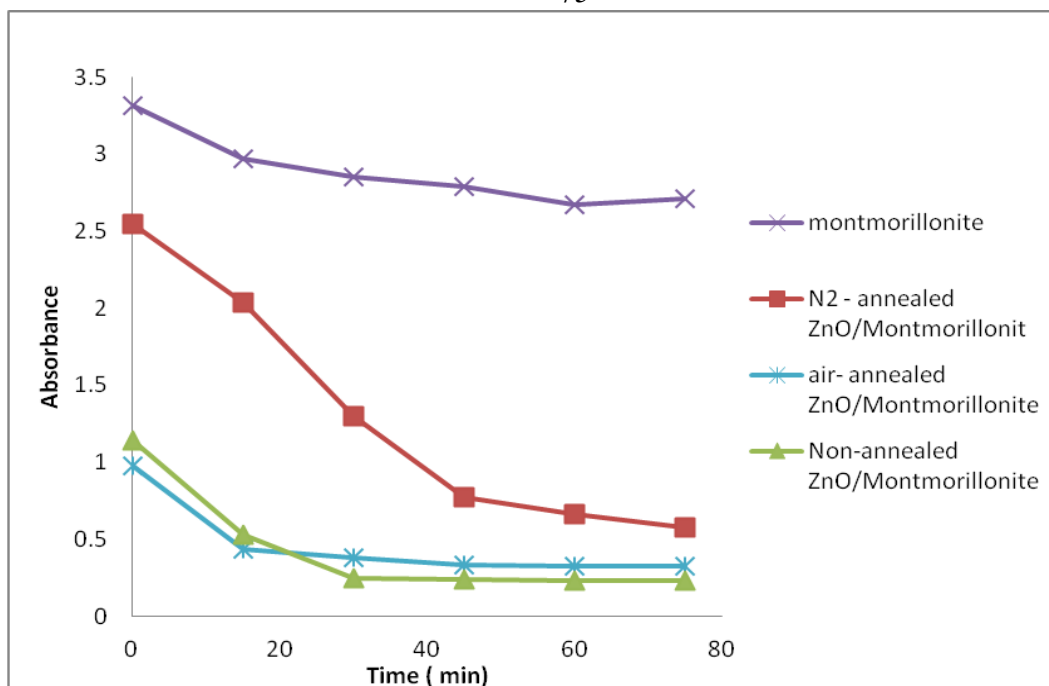


Figure 3.32: Photo-degradation of Tetracycline by different catalysts after adsorption equilibrium using (catalyst amount 0.1g, initial Tetracycline concentration 120 ppm, pH=7 and temperature 25°C under simulated solar light).

The photo-catalytic activities of raw Montmorillonite and ZnO/Montmorillonite are presented in Figure 3.32. From the Figure 3.32, adsorption of Tetracycline in dark on ZnO/Montmorillonite was higher than that on naked Montmorillonite. After adsorption, the remaining solution of Tetracycline was placed under light for 75 min and the results of removing Tetracycline after 15 min is described in Table 3.10.

Table 3.10: Values of percentage of photo-degradation, turnover number (TN), turnover frequency (TF) and quantum yield (QY) measured for Tetracycline degradation after 15 min with different type of composite catalyst.

| Amount of ZnO g (10^{-2}) | Catalyst Type | % Degradation | TN (10^{-3}) | TF (10^{-4}) | QY |
|----------------------------------|--------------------------|---------------|---------------------|---------------------|------|
| 6.7 | Non-annealed | 56 | 6.71 | 4.48 | 0.32 |
| 6.7 | air-annealed | 54 | 5.13 | 3.42 | 0.25 |
| 6.7 | N ₂ -annealed | 20 | 2.85 | 1.90 | 0.14 |
| 0 | Montmorillonite | 11 | - | - | 0.16 |
| 6.7 | ZnO | 5 | 1.64 | 0.11 | 0.08 |

However, it was found that the photo-catalytic efficiency of non-annealed ZnO/Montmorillonite is higher than the efficiencies of the other catalysts as can be seen from Table 3.9. This can be attributed to the higher number of oxygen molecules available in the surface of composite material structure. However, naked Montmorillonite has naturally trace amount of oxides as TiO₂ photo-oxidation, which may give it some activity toward photo-degradation of Tetracycline [80].

3.3.2.1 Effect of pH on Photo-degradation

The effect of pH on degradation of Tetracycline under simulated solar light, by using non-annealed ZnO/Montmorillonite catalyst, is illustrated in Figure 3.33.

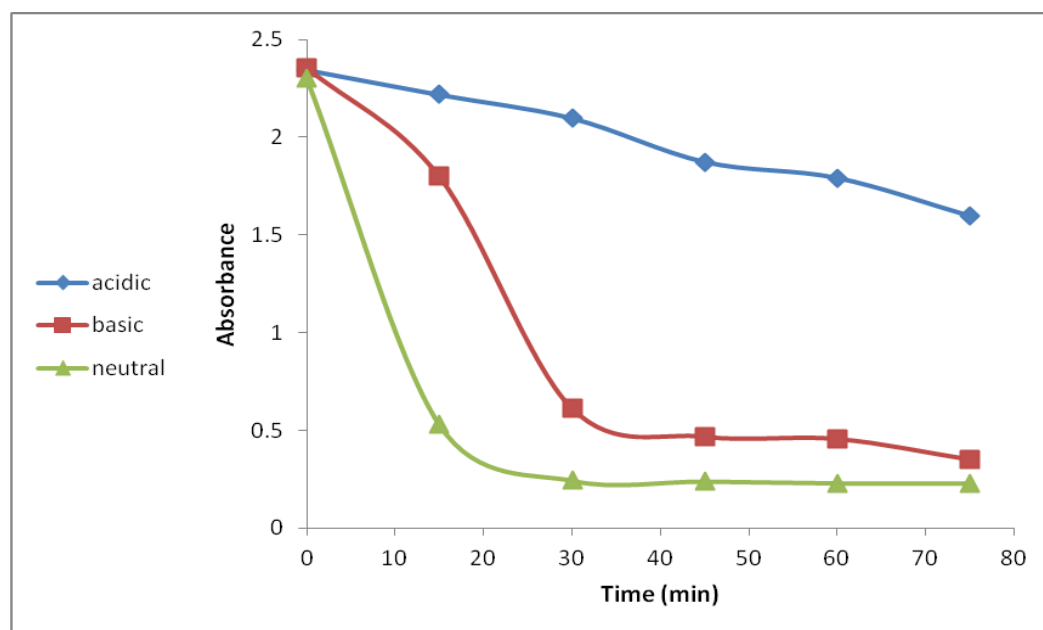


Figure 3.33: Effect of pH on degradation of Tetracycline with contact time using (non-annealed ZnO/Montmorillonite catalyst amount: 0.1 g, Tetracycline concentration: 120 ppm, and temperature: 25°C under simulated solar light.

The results of Figure (3.26) are summarized in Table 3.11. From the Table and the Figure, the values for degradation percentage, TF, TN and QY were higher in basic medium than in acidic medium. This means that the catalyst efficiency is higher at higher pH values. This is consistent with naked ZnO results, where photo-degradation reactions of Tetracycline became faster at higher pH.

Table 3.11: Values of percentage photo-degradation, turnover number (TN), turnover frequency (TF) and quantum yield (QY) measured for Tetracycline degradation by non-annealed ZnO/Montmorillonite after 15 min in different pH media.

| Amount of ZnO (10^{-2}) | pH | Degradation % | TN (10^{-3}) | TF (10^{-4}) | Q.Y |
|-----------------------------|---------------|---------------|------------------|------------------|------|
| 6.7 | acidic medium | 5.4 | 1.22 | 0.81 | 0.06 |
| 6.7 | basic medium | 23.5 | 5.25 | 3.50 | 0.25 |
| 6.7 | Neutral | 76.3 | 16.7 | 11.1 | 0.81 |

3.4 Recovery of ZnO/Montmorillonite Material

Recovery of photo-catalyst was studied by isolating the catalyst from the first experiment then reusing in another experiment (first recovery). Similar steps were followed to reuse for another time. Table 3.12 shows that percentage of degradation using first recovery was 77% with respect to using fresh catalyst. For second recovery, percentage recovery was 40% for same time. Therefore, catalysts can be recoverable and reused for more than one time. This indicates that catalysts are soundly stable and active, but the reactivity reduced in the second recovery. The results indicated that bonds between ZnO and Montmorillonite were strong enough to survive photo-catalytic reaction conditions. Before reusing of the catalyst, Specific solutions and conditions may be needed to clean Tetracycline from the surface of the composite material, as DMSO, in future work.

Table 3.12: Efficiency of recovered non-annealed ZnO/Montmorillonite in photo-degradation reaction of Tetracycline.

| Catalyst Sample | % Removal of Tetracycline |
|---------------------------------|----------------------------------|
| Fresh catalyst | 78 |
| 1st Recovered | 77 |
| 2nd Recovered | 40 |

Conclusion:

In the present work, ZnO/Montmorillonite was synthesized by a precipitation method. ZnO was supported onto the surface of Montmorillonite.

The ZnO/Montmorillonite composite material improves the physiochemical properties and photo-degradation of Tetracycline. Increased adsorption capacity of Montmorillonite helped to enhance the rate of photo-degradation reaction when ZnO was supported on it by synergic effect.

From the results of Tetracycline adsorption and photo-degradation reactions using ZnO and ZnO/Montmorillonite under different experimental conditions, we can draw the following conclusions:

- 1- Removal of Tetracycline by adsorption on ZnO/Montmorillonite is more effective than on naked Montmorillonite.
- 2- The rate of adsorption on ZnO/Montmorillonite composite material was not affected by temperature, and the process involved small activation energy with physisorption in neutral media.
- 3- Adsorption of Tetracycline on Montmorillonite and non- annealed ZnO/Montmorillonite followed a pseudo-second-order kinetics. Adsorption equilibrium could be reached after 120 min.

4- Adsorption of Tetracycline on non- annealed ZnO/Montmorillonite followed a Langmuir adsorption isotherm with the sorption maximum approaching 112.36 mg/g.

5- XRD analysis showed no d-spacing changes between different prepared ZnO/Montmorillonite samples.

6- Commercial ZnO, prepared ZnO and ZnO/Montmorillonite powders have been investigated as photo-catalysts for photo-degradation of Tetracycline in water under different conditions. Non-annealed ZnO/Montmorillonite showed highest photo-activity of Tetracycline degradation. Supported commercial ZnO on Montmorillonite was more efficient than naked ZnO or Montmorillonite under simulated solar light.

7- Adsorption process and photo-degradation of Tetracycline with ZnO/Montmorillonite were strongly affected by pH of the solution.

8- Commercial ZnO showed slightly higher efficiency than prepared ZnO under simulated solar light.

Recommendations for Future Work

- 1- Determine the surface area of composite materials by BET and acetic acid methods.
- 2- Further work needs to be made in order to study the lowering of the supported catalyst activity on reuse.
- 3- Prepare ZnO/Montmorillonite by mixing commercial ZnO with Montmorillonite rather than mixing Montmorillonite with Zinc acetate.
- 4- Do more kinetic study using the prepared ZnO/Montmorillonite catalyst system on photo-degradation of Tetracycline. Study the Effect of catalyst amount, temperature, recovery, ionic strength and hardness.
- 5- Further study of photo-degradation of Tetracycline by using ZnO nanoparticles prepared by different methods.
- 6- Study the effect of changing temperature and time of annealing on the adsorption and photo-degradation properties of ZnO/Montmorillonite composite material.
- 7- Study the mechanisms of photo-degradation of Tetracycline and the nature of bond between Tetracycline and composite material.
- 8- Separate the intermediate products of degradation and analysis by HPLC or GC-MS.

9- Prepare new types of composite material, such as ZnO/Kaolonite or ZnO/Natural local Clay, and study their effect of on Tetracycline removal.

10 - Determine the occurrence levels of Tetracycline in Palestinian drinking water.

References

- [1] I. Chopra, M. Roberts, **Tetracycline Antibiotics: Mode of Action, Applications, Molecular Biology, and Epidemiology of Bacterial Resistance**, *Microbiology and Molecular Biology Reviews*, **65** (2001) 232-260.
- [2] S.B. Levy, **The Challenge of Antibiotic Resistance**, *Scientific American*, **278** (1998) 32-39.
- [3] [Http://Www.Nlm.Nih.Gov/Medlineplus/Antibiotics.Html](http://www.nlm.nih.gov/medlineplus/antibiotics.html) (Accessed 10 Aug 2014).
- [4] B. Duff, **Presence of Tetracycline Antibiotics in Surface Water, A Study of the Presence/Absence of Tetracycline in the Raccoon River Watershed**.[Http://Www.Dmww.Com/Upl/Documents/Water-Quality/Lab-Reports/Lab-Studies/Presence-Of-Tetracycline-Antibiotics-In-Surface-Water.Pdf](http://www.dmww.com/Upl/Documents/Water-Quality/Lab-Reports/Lab-Studies/Presence-Of-Tetracycline-Antibiotics-In-Surface-Water.Pdf) (Accessed 10/7/214).
- [5] J.C. Chee-Sanford, R.I. Mackie, S. Koike, I.G. Krapac, Y.-F. Lin, A.C. Yannarell, S. Maxwell, R.I. Aminov, **Fate And Transport of Antibiotic Residues and Antibiotic Resistance Genes Following Land Application of Manure Waste**, *Journal of Environmental Quality*, **38** (2009) 1086-1108.

- [6] K.M Stauffenberg, **Evaluating Photolysis And Sorption of Antibiotics in Both Laboratory and Environmental Settings.** (Phd Thesis). University of North Carolina at Chapel Hill. 2007.
- [7] A. Watkinson, E. Murby, D. Kolpin, S. Costanzo, **The Occurrence of Antibiotics in an Urban Watershed: from Wastewater to Drinking Water,** *Science of the Total Environment*, **407** (2009) 2711-2723.
- [8] A. Eslami, S. Nasser, B. Yadollahi, A. Mesdaghinia, F. Vaezi, R. Nabizadeh, S. Nazmara, **Photocatalytic Degradation of Methyl Tert-Butyl Ether (Mtbe) in Contaminated Water by ZnO Nanoparticles,** *Journal of Chemical Technology and Biotechnology*, **83** (2008) 1447-1453.
- [9] X. Peng, L. Manna, W. Yang, J. Wickham, E. Scher, A. **Kadavanich, A.P. Alivisatos, Shape Control of CdSe Nanocrystals,** *Nature*, **404** (2000) 59-61.
- [10] Z. Zhang, K. Sun, B. Gao, G. Zhang, X. Liu, Y. Zhao, **Adsorption of Tetracycline on Soil and Sediment: Effects of pH and the Presence of Cu (II),** *Journal of Hazardous Materials*, **190** (2011) 856-862.
- [11] B. Cunha, J. Comer, M. Jonas, **The Tetracyclines,** *The Medical Clinics of North America*, **66** (1982) 293-302.
- [12] G.M. Eliopoulos, M.C. Roberts, **Tetracycline Therapy: Update,** *Clinical Infectious Diseases*, **36** (2003) 462-467.

- [13] K. Kümmerer, **Antibiotics in The Aquatic Environment—A Review—Part I**, *Chemosphere*, **75** (2009) 417-434.
- [14] X. Miao, F. Bishay, M. Chen, C.D. Metcalfe, **Occurrence of Antimicrobials In the Final Effluents of Wastewater Treatment Plants in Canada**, *Environmental Science & Technology*, **38** (2004) 3533-3541.
- [15] X. Xu, X. Li, **Sorption And Desorption Of Antibiotic Tetracycline On Marine Sediments**, *Chemosphere*, **78** (2010) 430-436.
- [16] A.R. Sapkota, F.C. Curriero, K.E. Gibson, K.J. Schwab, **Antibiotic-Resistant Enterococci and Fecal Indicators in Surface Water and Groundwater Impacted by a Concentrated Swine Feeding Operation**, *Environmental Health Perspectives*, **115** (2007) 1040.
- [17] F. Varanda, M.J. Pratas De Melo, A.I. Caço, R. Dohn, F.A. Makrydaki, E. Voutsas, D. Tassios, I.M. Marrucho, **Solubility of Antibiotics in Different Solvents. 1. Hydrochloride Forms of Tetracycline, Moxifloxacin, and Ciprofloxacin**, *Industrial & Engineering Chemistry Research*, **45** (2006) 6368-6374.
- [18] [Http://Www.Chm.Bris.Ac.Uk/Motm/Tetracycline/Tetracycline.Htm](http://Www.Chm.Bris.Ac.Uk/Motm/Tetracycline/Tetracycline.Htm), (Accessed 20/7/2014).
- [19] M.N. Rashed, " **Adsorption Technique for the Removal of Organic Pollutants from Water and Wastewater**, **Organic Pollutants -**

Monitoring, Risk and Treatment". Prof. M.Nageeb Rashed (Ed.), Isbn: 978-953-51-0948-8, InTech. (2013).

[20] A. Dąbrowski, **Adsorption—From Theory to Practice**, *Advances in a Colloid and Interface Science*, **93** (2001) 135-224.

[21] G.R. Rao." **Adsorption and Surface Catalytic Reactions, Advances in Physical Chemistry"**. T,Pradeer (Ed.), Isbn: 81-7023-950-8. (1999).

[22] E. Ruckenstein, D.C. Prieve, **Adsorption and Desorption of Particles and their Chromatographic Separation**, *AIChE Journal*, **22** (1976) 276-283.

[23] A. Mittal, **Adsorption Kinetics of Removal of a Toxic Dye, Malachite Green, from Wastewater by Using Hen Feathers**, *Journal of Hazardous Materials*, **133** (2006) 196-202.

[24] R.A. Figueroa, A. Leonard, A.A. Mackay, **Modeling Tetracycline Antibiotic Sorption to Clays**, *Environmental Science & Technology*, **38** (2004) 476-483.

[25] D. Avisar, O. Primor, I. Gozlan, H. Mamane, **Sorption of Sulfonamides and Tetracyclines to Montmorillonite Clay**, *Water, Air, & Soil Pollution*, **209** (2010) 439-450.

[26] M. Essington, J. Lee, Y. Seo, **Adsorption of Antibiotics by Montmorillonite and Kaolinite**, *Soil Science Society of America Journal*, **74** (2010) 1577-1588.

- [27] S.A. Sassman, L.S. Lee, **Sorption of Three Tetracyclines by Several Soils: Assessing the Role of pH and Cation Exchange**, *Environmental Science & Technology*, **39** (2005) 7452-7459.
- [28] D. Jia, D. Zhou, Y. Wang, H. Zhu, J. Chen, **Adsorption and Cosorption of Cu and Tetracycline on Two Soils with Different Characteristics**, *Geoderma Journal* , **146** (2008) 224-230.
- [29] L. Ji, W. Chen, L. Duan, D. Zhu, **Mechanisms for Strong Adsorption of Tetracycline to Carbon Nanotubes: A Comparative Study Using Activated Carbon and Graphite as Adsorbents**, *Environmental Science & Technology*, **43** (2009) 2322-2327.
- [30] Y. Gao, Y. Li, L. Zhang, H. Huang, J. Hu, S.M. Shah, X. Su, **Adsorption and Removal of Tetracycline Antibiotics from Aqueous Solution by Graphene Oxide**, *Journal of Colloid and Interface Science*, **368** (2012) 540-546.
- [31] A.E. Ciarlone, B.W. Fry, D.M. Ziemer, **Some Observations on the Adsorption of Tetracyclines to Glass and Plastic Labware**, *Microchemical Journal*, **42** (1990) 250-255.
- [32] W.Chen, C.Huang, **Adsorption and Transformation of Tetracycline Antibiotics with Aluminum Oxide**, *Chemosphere*, **79** (2010) 779-785.
- [33] D.Misra, **Adsorption and Orientation of Tetracycline on Hydroxyapatite**, *Calcified Tissue International*, **48** (1991) 362-367.

- [34] C. Gu, K. Karthikeyan, K.Sibley, J. Pedersen, J. A. **Sorption of the Antibiotic Tetracycline to Humic-Mineral Complexes**, *Journal of Environmental Quality*, **37** (2008) 704-711.
- [35] A. Caroni, C. De Lima, M. Pereira, J. Fonseca, **The Kinetics of Adsorption of Tetracycline on Chitosan Particles**, *Journal of Colloid And Interface Science*, **340** (2009) 182-191.
- [36] Y. Zhao, J. Geng, X. Wang, X. Gu, S. Gao, **Adsorption of Tetracycline onto Goethite in the Presence of Metal Cations and Humic Substances**, *Journal of Colloid and Interface Science*, **361** (2011) 247-251.
- [37] P.Chang, Z. Li, T. Yu, S. Munkhbayer, T. Kuo, Y. Hung, J. Jean, K.-H. Lin, **Sorptive Removal of Tetracycline from Water by Palygorskite**, *Journal of Hazardous Materials*, **165** (2009) 148-155.
- [38] L.Duong, **the Morphology and Structure of Intercalated and Pillared Clays**, (Phd. Thesis),Queensland University of Technology, Brisbane, 2008.
- [39] S. Guggenheim, R. Martin, **Definition of Clay and Clay Mineral: Joint Report of the AIPEA Nomenclature and CMS Nomenclature Committees**, *Clays and Clay Minerals*, **43** (1995) 255-256.
- [40] F. Bergaya, G. Lagaly, **General Introduction: Clays, Clay Minerals, and Clay Science**, *Handbook of Clay Science*, Elsevier, **1** (2006) 1-18.

- [41] M.C. Floody, B. Theng, P. Reyes, M. Mora, **Natural Nanoclays: Applications and Future Trends—A Chilean Perspective**, *Clay Minerals*, **44** (2009) 161-176.
- [42] J. Lory, Structure of Clays, **The Cooperative Soil Survey**, [Http://Soils.Missouri.Edu/Tutorial/Page8.Asp](http://Soils.Missouri.Edu/Tutorial/Page8.Asp) (Accessed 4/7/214).
- [43] B. Janczuk, T. Bialopiotrowicz, **Components of Surface Free Energy of Some Clay Minerals**, *Clays and Clay Minerals*, **36** (1988) 243-248.
- [44] T. Buehrer, **Role of Chemical Properties of Clays in Soil Science**, *Bulletin*, *Clays and Clay Minerals*, **1** (1952) 167-176.
- [45] T.A. Wolfe, T. Demirel, E.R. Baumann, **Interaction of Aliphatic Amines with Montmorillonite to Enhance Adsorption of Organic Pollutants**, *Clays and Clay Minerals*, **33** (1985) 301-311.
- [46] O. Abollino, M. Aceto, M. Malandrino, C. Sarzanini, E. Mentasti, **Adsorption of Heavy Metals on Na-Montmorillonite. Effect of pH and Organic Substances**, *Water Research*, **37** (2003) 1619-1627.
- [47] G.W. Bailey, J.L. White, T. Rothberg, **Adsorption of Organic Herbicides by Montmorillonite: Role of pH and Chemical Character of Adsorbate**, *Soil Science Society of America Journal*, **32** (1968) 222-234.

- [48] C. Wang, L. Juang, T. Hsu, C. Lee, J. Lee, F. Huang, **Adsorption of Basic Dyes onto Montmorillonite**, *Journal of Colloid and Interface Science*, **273** (2004) 80-86.
- [49] P.T. Hang, G. Brindley, **Methylene Blue Absorption by Clay Minerals. Determination of Surface Areas and Cation Exchange Capacities (Clay-Organic Studies Xviii)**, *Clays And Clay Minerals*, **18** (1970) 203-212.
- [50] L.A. Pinck, **Adsorption of Proteins, Enzymes and Antibiotics by Montmorillonite**, *Clays and Clay Minerals*, **9** (1962) 520-529.
- [51] M.E. Parolo, M. Savini, J. Vallés, M. Baschini, M. Avena, **Tetracycline Adsorption on Montmorillonite: pH and Ionic Strength Effects**, *Applied Clay Science*, **40** (2008) 179-186.
- [52] W.F. Hower, **Adsorption of Surfactants on Montmorillonite**, *Clays and Clay Mineral*, **18** (1970) 97-105.
- [53] B. Damardji, H. Khalaf, L. Duclaux, B. David, **Preparation of TiO₂ pillared Montmorillonite as Photocatalyst Part I. Microwave Calcination, Characterisation, and Adsorption of A Textile Azo Dye**, *Applied Clay Science*, **44** (2009) 201-205.
- [54] G.K. Zhang, X.M. Ding, F.S. He, X.Y. Yu, J. Zhou, Y.J. Hu, J.W. Xie, **Low-Temperature Synthesis and Photocatalytic Activity of TiO₂ Pillared Montmorillonite**, *Langmuir*, **24** (2008) 1026-1030.

- [55] V. Parmon, A. Emeline, N. Serpone, **Glossary of Terms in Photocatalysis and Radiocatalysis**, *International Journal of Photoenergy*, **4** (2002) 91-131.
- [56] M.R. Hoffmann, S.T. Martin, W. Choi, D.W. Bahnemann, **Environmental Applications of Semiconductor Photocatalysis**, *Chemical Reviews*, **95** (1995) 69-96.
- [57] A. Kudo, **Photocatalyst Materials for Water Splitting**, *Catalysis Surveys from Asia*, **7** (2003) 31-38.
- [58] [Http://Dev.Nsta.Org/Evwebs/1952/Photocatalysis.Htm](http://Dev.Nsta.Org/Evwebs/1952/Photocatalysis.Htm), (Accessed on 4/7/2014).
- [59] A. Janotti, C.G. Van De Walle, **Fundamentals of Zinc Oxide as A Semiconductor**, *Reports on Progress in Physics*, **72** (2009) 126501.
- [60] J. Portier, H. Hilal, I. Saadeddin, S. Hwang, M. Subramanian, G. Campet, **Thermodynamic Correlations and Band Gap Calculations in Metal Oxides**, *Progress in Solid State Chemistry*, **32** (2004) 207-217.
- [61] H.E. Brown, " **Zinc Oxide: Properties and Applications**, **International Lead Zinc**". Research Organization, New York, 1976.
- [62] N.N. Greenwood, A. Earnshaw: "**Chemistry of the Elements**", Pergamon Press Oxford Etc., 1984.

- [63] K. Biswas, M.-H. Du, **Ax Centers In Ii-Vi Semiconductors: Hybrid Functional Calculations**, *Applied Physics Letters*, **98** (2011) 181913.
- [64] K. Takahashi, A. Yoshikawa, A. Sandhu: "**Wide Bandgap Semiconductors: Fundamental Properties and Modern Photonic and Electronic Devices**", Springer Berlin Heidelberg, 2007.
- [65] I. Fatimah, S. Wang, D. Wulandari, **Zno/Montmorillonite for Photocatalytic and Photochemical Degradation of Methylene Blue**, *Applied Clay Science*, **53** (2011) 553-560.
- [66] R.F. Gibson : "**Principles of Composite Material Mechanics**", 3rd Edition, Crc Press, 2011.
- [67] S.V. Pathak, **Enhanced Heat Transfer in Composite Materials**, (Master's Thesis).Ohio University, Athens, USA. 2013.
- [68] K.K. Choy, J.F. Porter, G. Mckay, **Single and Multicomponent Equilibrium Studies for the Adsorption of Acidic Dyes on Carbon from Effluents**, *Langmuir*, **20** (2004) 9646-9656.
- [69] J. He, S. Hong, L. Zhang, F. Gan, Y. Ho, **Equilibrium and Thermodynamic Parameters of Adsorption of Methylene Blue onto Rectorite**, *Fresenius Environmental Bulletin*, **19** (2010) 2651-2656.
- [70] R.I. Masel: "**Principles of Adsorption and Reaction on Solid Surfaces**". Wiley, New York, 1996.

- [71] H. Qiu, L. Lv, B. Pan, Q. Zhang, W. Zhang, Q. Zhang, **Critical Review in Adsorption Kinetic Models**, *Journal of Zhejiang University Science A*, **10** (2009) 716-724.
- [72] D. Sridev, K. Rajendran, **Synthesis and Optical Characteristics of ZnO Nanocrystals**, *Bulletin of Materials Science*, **32** (2009) 165-168.
- [73] S.A.H. Hejjawi, **TiO₂ and ZnO Photocatalysts for Degradation of Widespread Pharmaceutical Wastes: Effect of Particle Size and Support**, (Master's Thesis), An-Najah National University, Nablus, Palestine, 2013.
- [74] [Http://Www.BeilsteinJournals.Org/Bjnano/Single/Articlefulltext.Htm? Publicid=2190-4286-5-62](http://www.beilsteinjournals.org/bjnano/single/articlefulltext.htm?publicid=2190-4286-5-62), (Accessed 12/8 2014).
- [75] F. Nouroozi, F. Farzaneh, **Synthesis and Characterization of Brush-Like ZnO Nanorods Using Albumen as Biotemplate**, *Journal of the Brazilian Chemical Society*, **22** (2011) 484-488.
- [76] M. Kondo, S. Adachi, **Optical Properties of NaCl: Sn²⁺ Phosphor Synthesized from Aqueous NaCl/SnCl₂/HCl Solution**, *ECS Journal of Solid State Science and Technology*, **2** (2013) R9-R15.
- [77] V. Drits, J. Srodon, D. Eberl, **XRD Measurement of Mean Crystallite Thickness of Illite and Illite/Smectite: Reappraisal of the Kubler Index and the Scherrer Equation**, *Clays and Clay Minerals*, **45** (1997) 461-475.

- [78] W. Bnarley, R. Gnru, **High Temperature Thermal Effects of Clay and Related Materials, State Geological Suraey**, (Jrbana, Illinois), (1951). Http://Www.Minsocam.Org/Ammin/Am36/Am36_182.Pdf, (Accessed On 1/7/2014).
- [79] M. Shamsudin, A. Suriani, S. Abdullah, S. Yahya, M. Rusop, **Impact of Thermal Annealing Under Nitrogen Ambient on Structural, Micro-Raman, and Thermogravimetric Analyses of Camphoric-Cnt**, *Journal of Spectroscopy*, 2013, (2012).
- [80] Y. Liu, X. Lu, F. Wu, N. Deng, **Adsorption and Photooxidation of Pharmaceuticals and Personal Care Products on Clay Minerals, Reaction Kinetics, Mechanisms and Catalysis**, **104** (2011) 61-73.
- [81] Z. Li, L. Schulz, C. Ackley, N. Fenske, **Adsorption of Tetracycline on Kaolinite iith pH-Dependent Surface Charges**, *Journal of Colloid and Interface Science*, **351** (2010) 254-260.
- [82] S. Babić, A.J. Horvat, D. Mutavdžić Pavlović, M. **Kaštelan-Macan**, **Determination of Pk_a Values of Active Pharmaceutical Ingredients**, *Trac Trends in Analytical Chemistry*, **26** (2007) 1043-1061.
- [83] L.S. Porubcan, C.J. Serna, J.L. White, S.L. Hem, **Mechanism of Adsorption of Clindamycin and Tetracycline by Montmorillonite**, *Journal of Pharmaceutical Sciences*, **67** (1978) 1081-1087.

- [84] H.K. Boparai, M. Joseph, D.M. O'carroll, **Kinetics and Thermodynamics of Cadmium Ion Removal by Adsorption onto Nano Zero Valent Iron Particles**, *Journal of Hazardous Materials*, **186** (2011) 458-465.
- [85] Y. Ho, G. Mckay, **Pseudo-Second Order Model for Sorption Processes**, *Process Biochemistry*, **34** (1999) 451-465.
- [86] D.G. Kinniburgh, **General Purpose Adsorption Isotherms**, *Environmental Science & Technology*, **20** (1986) 895-904.
- [87] M.A. Al-Anber : "**Thermodynamics Approach in the Adsorption of Heavy Metals**, Juan Carlos Moreno-Pirajan, **Thermodynamics-Interaction Studies-Solids**", Liquids and Gases Book, First Edition., In-Tech, Rijeka, (2011) 737-764.
- [88] S. Schneider, M.O. Schmitt, G. Brehm, M. Reiher, P. Matousek, M. Towrie, **Fluorescence Kinetics of Aqueous Solutions of Tetracycline and Its Complexes with Mg^{2+} And Ca^{2+}** , *Photochemical & Photobiological Sciences*, **2** (2003) 1107-1117.
- [89] A. Hamza, J. Fatuase, S. Waziri, O. Ajayi, **Solar Photocatalytic Degradation of Phenol Using Nanosized ZnO and A- Fe_2O_3** , *Journal of Chemical Engineering and Materials Science*, **4** (2013) 87-92.

- [90] N. Serpone, A. Salinaro, Terminology, **Relative Photonic Efficiencies and Quantum Yields in Heterogeneous Photocatalysis. Part I: Suggested Protocol**, *Pure and Applied Chemistry*, **71** (1999) 303-320.
- [91] J.-M. Herrmann, Heterogeneous **Photocatalysis: An Emerging Discipline Involving Multiphase Systems**, *Catalysis Today*, **24** (1995) 157-164.
- [92] R.A. Palominos, M.A. Mondaca, A. Giraldo, G. Peñuela, M. Pérez-Moya, H.D. Mansilla, **Photocatalytic Oxidation of the Antibiotic Tetracycline on TiO₂ and ZnO Suspensions**, *Catalysis Today*, **144** (2009) 100-105.
- [93] P.R. Gogate, A.B. Pandit, **A Review of Imperative Technologies for Wastewater Treatment I: Oxidation Technologies at Ambient Conditions**, *Advances in Environmental Research*, **8** (2004) 501-551.

جامعة النجاح الوطنية

كلية الدراسات العليا

دراسة التأثير المتبادل لحبيبات أكسيد الزنك النانوية المثبتة على المنتموريالونيت
وعملها كحفاز للتحطيم الضوئي وكمادة ممتزة للتراسيكلين

إعداد

نجاه ماهر نمر الدقة

إشراف

أ.د. حكمت هلال

د. وحيد الجندي

قدمت هذه الرسالة استكمالاً لمتطلبات الحصول على درجة الماجستير في الكيمياء بكلية
الدراسات العليا في جامعة النجاح الوطنية في نابلس، فلسطين.

2014

ب

دراسة التأثير المتبادل لحبيبات أكسيد الزنك النانوية المثبتة على المنتموريالونيت وعملها

كحافز للتحطيم الضوئي وكمادة ممتزة للنتراسيكلين

إعداد

نجاه ماهر نمر الدقة

إشراف

أ.د. حكمت هلال

د. وحيد الجندي

الملخص

الاستخدام الواسع النطاق للمضادات الحيوية في الأدوية البشرية والبيطرية أدى الى الكشف المتكرر عنها في التربة والمياه الجوفية ومياه الصرف الصحي. ويعتبر التحطيم الضوئي و الإمتزاز من أكثر الطرق فعالية في تنقية المياه من الملوثات مثل المضادات الحيوية. في هذا البحث أجرينا دراسة لإزالة مادة النتراسيكلين (وهو مضاد حيوي شائع الاستخدام) بواسطة أكسيد الزنك وبوساطة أكسيد الزنك المثبت على سطح المونتمورينوليت. وأكسيد الزنك من أشباه الموصلات وهو حافز لتفاعلات التحطيم الضوئي التي تستخدم لأكسدة الملوثات تحت ضوء الشمس الى مواد اكثر امانا. ذلك يرجع إلى أن أكسيد الزنك محفز منخفض التكلفة ويعمل تحت ظروف تفاعل معتدلة وفعالته في التحطيم الضوئي عالية.

يشكل المونتمورينوليت نوعا من الفخار ذي خصائص فيزيائية مميزة وهو معروف بكفاءته في امتزاز المضاد الحيوي النتراسيكلين كما تم ذكره في دراسات سابقة. في هذا العمل تم تثبيت أكسيد الزنك على سطح مونتمورينوليت ثم درس نشاط الحافز للتحطيم الضوئي تحت ضوء يحاكي الضوئي الشمسي، كما تم دراسة خاصية امتزاز النتراسيكلين ايضا. وقد تم استخدام قياسات مطيافية الوميض وتمثيل الاشعة السينية في دراسة خواص الحفازات والمواد المستخدمة سواء كانت تجارية ام محضرة في المختبر .

تم إجراء عملية امتزاز للنتراسايكلين على سطح المونتمورينوليت المستقل مرة، ومرة اخرى على سطح المونتموريلونيت المثبت عليه اكسيد الزنك تحت ظروف مختلفة مثل : درجة الحموضة،

ت

وقت الخلط وتركيز التتراسيكلين، تأثير الشبي ودرجة الحرارة، كما تم إجراء دراسة حركيات عملية الامتزاز. أظهرت النتائج أن عملية الامتزاز على سطح المونتمورينوليت المثبت عليه اكسيد الزنك (غير المشوي) يتبع لنموذج لانجموير مع سعة الامتزاز 112.36 ملغ / غرام عند الرقم الهيدروجيني المتعادل. وقد وجد أن قدرة امتصاص المونتمورينوليت المثبت عليه اكسيد الزنك هي أكثر منه في حالة المونتمورينوليت العاري بحوالي ضعفين. ولقد وجد أن اقصى فعالية للامتزاز حدثت عند وسط متعادل.

تم إجراء التحطيم الضوئي للتتراسيكلين بواسطة اكسيد الزنك التجاري تحت ظروف تفاعل مختلفة مثل : درجة الحموضة وتركيز التتراسيكلين وكمية الحفاز. وقد وجد أنه في الظروف القاعدية ارتفعت فعالية التحطيم الضوئي تحت الضوء المحاكي للضوء الشمسي. و تم أيضاً دراسة تأثير العوامل المختلفة على عمل المونتمورينوليت المثبت عليه اكسيد الزنك كحفاز للتحطيم الضوئي للتتراسيكلين.وقد وجد انه أكثر فعالية في درجة حموضة متعادلة.

